

1 **Evidence for an earlier greenhouse cooling effect in the**  
2 **stratosphere before the 1980s over the Northern**  
3 **Hemisphere**

4

5 **C. S. Zerefos<sup>1,2</sup>, K. Tourpali<sup>3</sup>, P. Zanis<sup>4</sup>, K. Eleftheratos<sup>5</sup>, C. Repapis<sup>1,10</sup>, A.**  
6 **Goodman<sup>6</sup>, D. Wuebbles<sup>7</sup>, I.S.A. Isaksen<sup>8</sup> and J. Luterbacher<sup>9</sup>**

7

8 [1] {Research Centre for Atmospheric Physics and Climatology, Academy of Athens, Athens,  
9 Greece}

10 [2] {Navarino Environmental Observatory (N.E.O.), Messinia, Greece}

11 [3] {Laboratory of Atmospheric Physics, Department of Physics, Aristotle University of  
12 Thessaloniki, Thessaloniki, Greece}

13 [4] {Department of Meteorology and Climatology, School of Geology, Aristotle University of  
14 Thessaloniki, Thessaloniki, Greece}

15 [5] {Laboratory of Climatology & Atmospheric Environment, University of Athens, Greece}

16 [6] {Department of Atmospheric Science, Colorado State University, Fort Collins, CO, USA}

17 [7] {Department of Atmospheric Sciences, University of Illinois, Urbana, IL, USA}

18 [8] {Department of Geosciences, University of Oslo, Oslo, Norway}

19 [9] {Climatology, Climate Dynamics and Climate Change, Department of Geography, Justus-  
20 Liebig University of Giessen, Germany}

21 [10] {Mariolopoulos-Kanaginis Foundation for the Environmental Sciences, Athens, Greece}

22

23 Correspondence to: C. S. Zerefos (zerefos@geol.uoa.gr)

24

25 Key words: stratospheric temperature, tropopause, trends, anthropogenic climate change,  
26 greenhouse warming and cooling

27

28

29 **Abstract**

30 This study provides a new look at the observed and calculated long-term temperature changes  
31 from the lower troposphere to the lower stratosphere since 1958 over the Northern  
32 Hemisphere. The datasets include the NCEP/NCAR reanalysis, the Free University of Berlin  
33 (FU-Berlin) and the RICH radiosonde datasets as well as historical simulations with the  
34 CESM1-WACCM global model participating in CMIP5. The analysis is mainly based on  
35 monthly layer mean temperatures derived from geopotential height thicknesses in order to  
36 take advantage from the use of the independent FU-Berlin stratospheric dataset of  
37 geopotential height data since 1957. This approach was followed to extend the records in the  
38 past for the investigation of the stratospheric temperature trends from the earliest possible  
39 time. After removing the natural variability with an autoregressive multiple regression model  
40 our analysis shows that the period 1958-2011 can be divided in two distinct sub-periods of  
41 long term temperature variability and trends; before and after 1980s. By calculating trends for  
42 the summer time to reduce interannual variability, the two periods are as follows. From 1958  
43 until 1979, non-significant trend ( $0.06 \pm 0.06$  °C/decade for NCEP) and slightly cooling trends  
44 ( $-0.12 \pm 0.06$  °C/decade for RICH) are found in the lower troposphere. The second period from  
45 1980 to the end of the records shows significant warming ( $0.25 \pm 0.05$  °C/decade for both  
46 NCEP and RICH). Above the tropopause a significant cooling trend is clearly seen in the  
47 lower stratosphere both in the pre-1980s period ( $-0.58 \pm 0.17$  °C/decade for NCEP,  $-0.30 \pm 0.16$   
48 °C/decade for RICH and  $-0.48 \pm 0.20$  °C/decade for FU-Berlin) and the post-1980s period ( $-$   
49  $0.79 \pm 0.18$  °C/decade for NCEP,  $-0.66 \pm 0.16$  °C/decade for RICH and  $-0.82 \pm 0.19$  °C/decade for  
50 FU-Berlin). The cooling in the lower stratosphere is a persistent throughout the year feature  
51 from the tropics up to 60° North. At polar latitudes competing dynamical and radiative  
52 processes are reducing the statistical significance of these trends. Model results are in line  
53 with re-analysis and the observations, indicating a persistent cooling ( $-0.33$  °C/decade) in the  
54 lower stratosphere during summer before and after the 1980s; a feature that is also seen  
55 throughout the year. However, the lower stratosphere CESM1-WACCM modelled trends are  
56 generally lower than re-analysis and the observations. The contrasting effects of ozone  
57 depletion at polar latitudes in winter/spring and the anticipated strengthening of the Brewer  
58 Dobson circulation from man-made global warming at polar latitudes are discussed. Our  
59 results provide additional evidence for an early greenhouse cooling signal in the lower  
60 stratosphere before the 1980s, which it appears well in advance relative to the tropospheric

61 greenhouse warming signal. The suitability for early warning signals in the stratosphere  
62 relative to the troposphere is supported by the fact that the stratosphere is less sensitive to  
63 changes due to cloudiness, humidity and man-made aerosols. Our analysis also indicates that  
64 the relative contribution of the lower stratosphere versus the upper troposphere low frequency  
65 variability is important for understanding the added value of the long term tropopause  
66 variability related to human induced global warming.

67

## 68 **1 Introduction**

69 Since the discovery of significant cooling trends in the lower stratosphere in the late 1970s,  
70 80s and 90s (Zerefos and Mantis, 1977; Angell and Korshover, 1983; Miller et al., 1992), a  
71 number of scientific articles have focused on the statistical space and time continuity of  
72 stratospheric temperature observations both from ground and from satellite retrievals. Those  
73 publications indicate that the lower stratosphere cooling continues from the 1980s to the  
74 present (Santer et al., 1999; Randel et al., 2009; WMO, 2011; Santer et al., 2013).

75 Common features in lower-stratospheric temperature change are found in all available  
76 radiosonde and satellite datasets<sup>1</sup>. One common finding is that in the global mean, the lower  
77 stratosphere has cooled by about  $-0.5$  °C/decade since 1980. Randel et al. (2009) reported that  
78 lower stratosphere cooling is a robust result over much of the globe for the period 1979–2007,  
79 being nearly uniform over all latitudes outside of the polar regions, with some differences  
80 among various radiosonde and satellite data sets. Substantially larger cooling trends are  
81 observed in the Antarctic lower stratosphere during spring and summer, in association with  
82 the development of the Antarctic ozone hole (Randel et al., 2009; Santer et al., 2013). In the  
83 tropical lower stratosphere the observations show significant long-term cooling (70–30 hPa)  
84 for 1979–2007, while less overall cooling is seen at 100 hPa (Randel et al., 2009). The global-  
85 mean lower stratospheric cooling has not occurred linearly, but stems from two downward  
86 steps in temperature, both of which are coincident with the cessation of transient warming  
87 after the volcanic eruptions of El Chichón and Mt. Pinatubo (Thompson and Solomon, 2009;  
88 Free and Lanzante, 2009). It should be also noted that the global mean lower stratospheric  
89 temperatures during the period following 1995 are significantly lower than they were during

---

<sup>1</sup> Today, there are six available global lower-stratospheric temperature data sets based on radiosonde data since the late 1950s; RATPAC (Free et al., 2005); HadAT (Thorne et al., 2005); RATPAC-lite (Randel and Wu, 2006); RAOBCORE (Haimberger, 2007); RICH (Haimberger et al., 2008); and IUK (Sherwood et al., 2008) and three satellite datasets; UAH (Christy et al., 2003); RSS (Mears and Wentz, 2009); and STAR, (Zou et al., 2009).

90 the decades prior to 1980, but have not dropped further since 1995 (WMO, 2011). Recently,  
91 Thompson et al. (2012) reported that the SSU data reprocessed by NOAA indicate stronger  
92 cooling trends in the middle and higher stratosphere than previously estimated, which cannot  
93 be captured by the available simulations with coupled chemistry–climate models (CCMs) and  
94 coupled atmosphere–ocean global climate models (AOGCMs). This global lower stratosphere  
95 cooling since the 1980s is also evident in the pre-satellite era with a cooling rate of  $\sim 0.35$   
96  $^{\circ}\text{C}/\text{decade}$  since 1958 (WMO, 2011). Randel et al., (2009) questioned the validity of the  
97 trends for the period 1958–1978 because of the sparse observational database and the known  
98 instrumental uncertainties for this period, together with the large trend uncertainties implied  
99 by the spread of results. Furthermore in other studies it was pointed out that the radiosonde  
100 datasets are not fully independent and that there are systematic biases in a number of stations  
101 relative to the satellites (Randel and Wu, 2006; Free and Seidel, 2007). These systematic  
102 biases are not well understood. Nevertheless, the different statistical approaches applied for  
103 homogenization are useful to assessing the overall uncertainty of the long-term stratospheric  
104 temperature trend estimates since the late 1950s (WMO, 2011).

105 The primary radiative forcing mechanisms responsible for global temperature changes in the  
106 stratosphere since 1979 have been increases in well-mixed GHG concentrations, increases in  
107 stratospheric water vapour, the decrease in stratospheric ozone primarily related to chlorine  
108 and bromine from various halocarbons, the effects of aerosols from explosive volcanic  
109 eruptions, and the effects of solar activity changes (e.g., Shine et al., 2003; Ramaswamy et al.,  
110 2006; WMO, 2007; IPCC, 2007; IPCC, 2013). The effects of volcanic eruptions, variations in  
111 solar radiation, and other sources of natural variability, including the wave-driven quasi-  
112 biennial oscillation (QBO) in ozone, can be accounted for through the use of indices in time  
113 series trends analyses (Tiao et al., 1990; Staehelin, 2001; Reinsel et al., 2005; Fioletov, 2009).  
114 However, the attribution of past lower stratosphere temperature trends is complicated by the  
115 effects of the increases and leveling off, of ozone depleting substances (ODSs) and the inter-  
116 annual to decadal variability of the Brewer-Dobson (BD) circulation.

117 The expectation of an accelerated and stronger BD circulation in a warmer climate is  
118 consistent with results from transport chemistry climate model simulations, wherein the lower  
119 stratospheric temperature trends may result from increases in upwelling over the tropical  
120 lower stratosphere and strengthening of the BD circulation (Rind et al., 2001; Cordero and  
121 Forster, 2006; Butchart et al., 2006; 2010; Austin and Li, 2006; Rosenlof and Reid, 2008;  
122 Garcia and Randel, 2008; Lamarque and Solomon, 2010). Unfortunately the detection of

123 trends in the BD circulation in observations is complicated because trends in BD circulation  
124 are small from 1980s through 2010 but are expected to become larger in the next few decades  
125 (Butchart, 2014). In addition, the BD circulation is not a directly observed physical quantity  
126 (WMO, 2011). Yet, observational evidence of an accelerated BD has been shown in a number  
127 of studies over both the tropics (e.g., Thompson and Solomon, 2005, Rosenlof and Reid,  
128 2008) and the high latitudes (Johanson and Fu, 2007; Hu and Fu, 2009; Lin et al., 2009; Fu et  
129 al., 2010). Thompson and Solomon (2009) have shown that the contrasting latitudinal  
130 structures of recent stratospheric temperature and ozone trends are consistent with the  
131 assumption of increases in the stratospheric overturning BD circulation. Also Free (2011)  
132 pointed out that trends in the tropical stratosphere show an inverse relationship with those  
133 over the Arctic for 1979–2009, which might be related to changes in stratospheric circulation.  
134 In contrast, other studies using balloon-borne measurements of stratospheric trace gases over  
135 the past 30 years to derive the mean age of air from sulfur hexafluoride (SF<sub>6</sub>) and CO<sub>2</sub> mixing  
136 ratios, found no indication of an increasing meridional circulation (Engel et al., 2009).  
137 Furthermore, Iwasaki et al. (2009) pointed out that the yearly trends in BD strength,  
138 diagnosed from all re-analyses products over the common period 1979–2001, are not reliably  
139 observed due to large diversity among the reanalyses. According to Randel and Thompson  
140 (2011), since there are no direct measurements of upwelling near the tropical tropopause, and  
141 there are large uncertainties in indirect measurements or assimilated data products (Iwasaki et  
142 al., 2009), temperature and ozone observations at the tropics can provide a sensitive measure  
143 of upwelling changes in the real atmosphere. In a recent article, Kawatani and Hamilton  
144 (2013) reported that a weakening trend in the lower stratosphere QBO amplitude provides  
145 strong support for the existence of a long-term trend of enhanced upwelling near the tropical  
146 tropopause.

147 The tropospheric warming and stratospheric cooling associated also with human forcing  
148 factors are expected to influence their interface i.e. the tropopause region (Santer et al., 2003a;  
149 Santer et al., 2003b; Seidel and Randel 2006; Son et al., 2009). Seidel and Randel (2006)  
150 examined global tropopause variability on synoptic, monthly, seasonal, and longer-term  
151 timescales using 1980–2004 radiosonde data and reported upward tropopause height trends at  
152 almost all of the (predominantly extratropical) stations analysed, yielding an estimated global  
153 trend of  $64 \pm 21$  m/decade. They reported that on multidecadal scale the change of the  
154 tropopause height is more sensitive to stratospheric temperature changes than to changes in  
155 the troposphere over both the tropics and the extratropics. Furthermore, Son et al. (2009)  
156 analysed a set of long-term integrations with stratosphere-resolving chemistry climate models,

157 reported that at northern mid-latitudes, long-term tropopause increase is dominated by the  
158 upper troposphere warming. Over the tropics and the southern hemisphere extratropics, the  
159 long-term tropopause trend is almost equally affected by both the trend in the lower  
160 stratosphere and the warming in the upper troposphere (Son et al., 2009).

161 A major open question that still remains to be answered is if the stratosphere can be  
162 considered as a more suitable region than the troposphere to detect anthropogenic climate  
163 change signals and what can be learned from the long-term stratospheric temperature trends.  
164 Indeed the signal-to-noise ratio in the stratosphere is, radiatively speaking, more sensitive to  
165 anthropogenic GHGs forcing and less disturbed from natural variability of water vapour and  
166 clouds when compared to the troposphere. This is because (a) the dependence of the  
167 equilibrium temperature of the stratosphere on CO<sub>2</sub> is larger than that on tropospheric  
168 temperature, (b) the equilibrium temperature of the stratosphere depends less upon  
169 tropospheric water vapour variability and (c) the influence of cloudiness upon equilibrium  
170 temperature is more pronounced in the troposphere than in the stratosphere where the  
171 influence decreases with height (Manabe and Weatherald, 1967). Furthermore, anthropogenic  
172 aerosols are mainly spread within the lower troposphere (He et al., 2008), and presumably  
173 have little effect on stratospheric temperatures.

174 Another open question is if the lower stratosphere started cooling since the time a reasonable  
175 global network became available i.e. after the International Geophysical Year (IGY) in 1957-  
176 1958. Such a long lasting cooling from the 60s until today needs to be re-examined and  
177 explained. To what extent are the cooling trends in the lower stratosphere related to human  
178 induced climate change? Has it been accelerating, for instance at high latitudes in  
179 winter/spring due to ozone depletion? Has it been interrupted by major volcanic eruptions and  
180 El Nino events (Zerefos et al., 1992) or large climatological anomalies?

181 The study addresses those questions and presents a new look at observed temperature trends  
182 over the Northern Hemisphere from the troposphere up to the lower stratosphere in a search  
183 for an early warning signal of global warming i.e. a cooling in the lower stratosphere relative  
184 to the warming in the lower atmosphere.

185

## 186 **2 Data and analysis of the statistical methods**

### 187 **2.1 Data**

188 Tropospheric and stratospheric temperature, pressure and geopotential height data used in this

189 study are based on the following sources: a) the NCEP/NCAR reanalysis I product (NCEP)  
190 data from 1958 to 2011 (Kalnay et al., 1996; Kistler et al., 2001), b) the Free University of  
191 Berlin (FU-Berlin) from 1958 to 2001, c) the Radiosonde Innovation Composite  
192 Homogenization (RICH) data (Haimberger, 2007; Haimberger et al., 2008) from 1958 to 2006  
193 and d) historical simulations with the NCAR Community Earth System Model (CESM)  
194 coupled to the "high-top" Whole Atmosphere Community Climate Model (WACCM)  
195 CESM1-WACCM (Marsh et al., 2013) from 1958 to 2005. Our analysis is focused at the  
196 northern hemisphere, as the data coverage in the pre-satellite era has been denser there than at  
197 the southern hemisphere.

198 The FU-Berlin is an independent stratospheric analysis dataset which is based on earlier  
199 subjective hand analyses of temperature and geopotential height fields at 50, 30 and 10 hPa  
200 for the northern hemisphere, using the 00UT radiosonde reports from the observational  
201 network by a team of experienced meteorologists (<http://www.geo.fu-berlin.de/en/met/ag/strat/produkte/fubdata/index.html>). Hydrostatic and geostrophic balances  
202 were assumed, and observed winds were used to guide the height and temperature analyses.  
203 The imposition of these balance conditions ensures a consistent dataset. In addition temporal  
204 continuity is assured by meteorological control. Note that these balance conditions can result  
205 in layer temperatures that deviate from the local radiosonde reports, which include meso-scale  
206 structures as well as any random or systematic observational errors (Labitzke et al., 2002;  
207 Manney et al., 2004). Earlier studies using the FU-Berlin dataset point that the approximate  
208 geostrophic balance of the upper winds ensures that the contour analysis will be more  
209 representative than the temperature analysis based on scattered radiosonde locations (Zerefos  
210 and Mantis, 1977; Mantis and Zerefos, 1979). The FU-Berlin analyses thus represent the  
211 synoptic-scale structure of the lower and middle stratosphere and the layer-mean temperature  
212 derived from the thickness is well suited for an investigation of large-scale climatic  
213 fluctuations of temperature. The analyses are provided as gridded data sets with a horizontal  
214 resolution of  $10^{\circ} \times 10^{\circ}$  before 1973, and  $5^{\circ} \times 5^{\circ}$  thereafter. FU-Berlin geopotential height data  
215 are available from July 1957 until December 2001 at 100, 50, and 30 hPa (Labitzke et al.,  
216 2002). Hence, from the FU-Berlin dataset we calculated layer-mean temperatures for the two  
217 lower stratospheric layers, 100-50 hPa and 50-30 hPa. It should be noted that the FU-Berlin  
218 dataset provides geopotential height data already since 1957, but temperature at the same  
219 levels since 1964. Hence, aiming in this study at presenting the stratospheric temperature  
220 trends from the earliest possible time, we have used the independent FU-Berlin stratospheric  
221 dataset with layer-mean temperature derived from geopotential heights thus extending the  
222

223 records in the past. The variability and trends derived using this dataset have been compared  
224 in the past to stratospheric data from other sources, both observations and reanalysis. The  
225 overall comparison is good, with differences in the variability (in the earlier period before  
226 1980) that can be attributed mainly to the close match between the FU-Berlin analysis and the  
227 radiosonde observations (e.g. Randel et al., 2009; Labitzke and Kunze, 2005; Manney et al.,  
228 2004; Randel et al, 2004; also in Labitzke et al., 2002 and references therein).

229 According to WMO (2011) large differences and continuity problems are evident in the  
230 middle and upper stratosphere within the reanalysis data sets, implying that trend analysis of  
231 stratospheric temperatures for the whole time period should be considered with caution  
232 (WMO, 2011). Aware of these problems, we opted to use here not the NCEP product of  
233 stratospheric temperature derived at specific atmospheric pressure levels, but rather the layer-  
234 mean temperature derived from the thickness of stratospheric and tropospheric layers (based  
235 on the geopotential height differences between specific atmospheric pressure levels) for  
236 comparison purposes with the respective quantities of the FU-Berlin dataset. Differences of  
237 monthly mean geopotential heights were used at standard atmospheric levels to derive the  
238 layer thickness and subsequently the layer mean temperature. For the NCEP dataset we have  
239 used the layers 1000-925 hPa (planetary boundary layer), 925-500 hPa (free troposphere),  
240 500-300 hPa (upper troposphere), 100-50 hPa and 50-30 hPa (lower stratosphere). The layer-  
241 mean temperatures were then used to calculate the averaged layer mean temperature over the  
242 latitude belts: northern polar (90N-60N), northern mid-latitudes (60N-30N) and the northern  
243 tropics (30N-5N). Furthermore, we also used in our analysis the tropopause pressure from  
244 NCEP to study the interannual correlation of tropopause pressure with tropospheric and  
245 stratospheric temperatures.

246 In our analysis we have used simulations with CESM1-WACCM, a state-of-the-art "high top"  
247 chemistry climate model coupled to the earth system model CESM that extends from the  
248 surface to  $5.1 \times 10^{-6}$  hPa (approximately 140 km). It has 66 vertical levels and horizontal  
249 resolution of  $1.9^\circ$  latitude by  $2.5^\circ$  longitude. The historical simulations with CESM1-WACCM  
250 were carried out as part of phase 5 of the Coupled Model Intercomparison Project (CMIP5).  
251 CESM1-WACCM has an active ocean and sea ice components as described by Holland et al.  
252 (2012). As shown in Marsh et al. (2013) for CESM1-WACCM, an updated parameterization  
253 of non-orographic gravity waves led to an improvement in the frequency of northern  
254 hemisphere (NH) sudden stratospheric warmings (SSWs). Furthermore the model also  
255 includes a representation of the QBO leading to a significant improvement in the

256 representation of ozone variability in the tropical stratosphere compared to observations. The  
 257 model's chemistry module is based on version 3 of the Model for OZone And Related  
 258 chemical Tracers (Kinnison et al. 2007). Volcanic aerosol surface area density in WACCM is  
 259 prescribed from a monthly zonal mean time series derived from observations including the  
 260 following major volcanic eruptions in historical simulations: Krakatau (1883), Santa Maria  
 261 (1902), Agung (1963), El Chichón (1982), and Pinatubo (1991). WACCM explicitly  
 262 represents the radiative transfer of the greenhouse gases CO<sub>2</sub>, CH<sub>4</sub>, N<sub>2</sub>O, H<sub>2</sub>O, CFC-12 and  
 263 CFC-11 (which includes also additional halogen species). WACCM simulation used here was  
 264 performed with all observed forcing from 1955-2005. The observed forcing included changes  
 265 in surface concentrations of radiatively active species, daily solar spectral irradiance, volcanic  
 266 sulfate heating and the QBO. A more detailed description of the CESM1-WACCM historical  
 267 simulations can be found in Marsh et al. (2013).

268 As each source of analysis/reanalysis data spans over a different period, the time series were  
 269 deseasonalized for the period of 1961-1990, common to all data sets. The same procedure was  
 270 followed for the tropopause pressure. The RICH dataset was used at the standard atmospheric  
 271 levels. The temperature anomalies from the RICH dataset available at standard pressure levels  
 272 were adjusted accordingly. Finally, it should be noted that the selection of various time  
 273 periods is related to the different time periods of the used datasets aiming to a more  
 274 representative comparison among them.

275

## 276 **2.2 Analysis of methods**

277 A multiple linear regression time series analysis with an autoregressive statistical model is  
 278 applied on the deseasonalized time series of zonally averaged layer mean temperature  
 279 similarly to the statistical approach applied by Reinsel et al. (2005). The regression model is  
 280 of the form:

$$281 \quad M(t) = \alpha_0 + \alpha_1 t + \sum g_i Z_i + N(t); 0 < t \leq T \quad (1)$$

282 Where  $M(t)$  is the monthly deseasonalized zonal mean temperature and  $t$  is the time in  
 283 months with  $t = 0$  corresponding to the initial month and  $t = T$  corresponding to the last  
 284 month.

285 The term  $\alpha_0$  is an overall level term while  $\alpha_1$  accounts for a linear trend. The terms  $g_i Z_i$  in the  
 286 statistical model reflect the temperature variability related to the natural variability, where  $Z_i$   
 287 represent a number of climatic and dynamical indices and  $g_i$  are the respective regression

288 coefficients. Specifically the climatic and dynamical indices used here include the 11-year  
289 solar cycle (using the solar F10.7 radio flux as a proxy), plus two orthogonal time series to  
290 model QBO, namely the standardized zonal wind at 30hPa and 50hPa (e.g., Crooks and Gray,  
291 2005, Austin et al., 2009).

292 It is well known that significant transient warming events occurred in the stratosphere  
293 following the volcanic eruptions of Agung (March 1963), El Chichon (April 1982) and Mount  
294 Pinatubo (June 1991), and these can substantially influence temperature trend estimates  
295 (especially if the volcanic events occur near either end of the time series in question). The  
296 common approach in order to avoid a significant influence on trend results is to omit data for  
297 2 years following each eruption in the regression analysis. In order to investigate the role  
298 played by stratospheric aerosols, we include terms to account for the influence of  
299 stratospheric aerosol variability, using the Stratospheric Aerosol Optical Depth (Sato et al.,  
300 1993) as an index in the regression model.

301 Finally,  $N(t)$  is the unexplained noise term. The statistical model is first-order autoregressive  
302 (AR(1)), and the term  $N(t)$  satisfies:

$$303 \quad N(t) = \phi N(t-1) + e(t) \quad (2)$$

304 where  $e(t)$  is an independent random variable with zero mean, commonly known as the white  
305 noise residuals. This AR(1) model allows for the noise to be (auto)correlated among  
306 successive measurements and is typically positive for data which show smoothly varying  
307 changes (naturally occurring) in  $N(t)$  over time (Reinsel, 2002).

308 The temperature trends and the role played by the various climatic and dynamic factors  
309 described above are examined in detail. The focus is on the detection of trends before and  
310 after the beginning of the satellite era (i.e. 1979), a period that is also the benchmark for  
311 ozone depletion.

312

### 313 **3 Results**

#### 314 **3.1 Summer and year-round trends**

315 In the summer, the stratosphere is less disturbed because it is characterised by lower vertically  
316 propagating wave activity from the troposphere, it has smaller natural variability than winter  
317 (Webb, 1966; Berger and Lübken, 2011; Gettelman et al., 2011) and it is also not influenced  
318 by chemical ozone depletion due to ODSs at high latitudes. Hence the less “noisy” summer

319 records offer the opportunity to investigate for better estimates of the lower stratospheric  
320 temperature trends. Figure 1 presents the time series of the layer mean temperatures in  
321 summer (June-July-August) for the northern hemisphere at tropical, mid and higher latitudinal  
322 zones from the lower troposphere up to the stratosphere, calculated from NCEP reanalysis,  
323 FU-Berlin and RICH datasets. The thick black lines represent the linear trends before and  
324 after 1980, a year that marks the beginning of the availability of satellite data whose inclusion  
325 resulted to increased global coverage. Figure 1 shows a consistent cooling of the lower  
326 stratosphere in NCEP, FU-Berlin and RICH datasets that persists in both pre- and post-80s  
327 periods. Specifically, for the period 1958-1979, there is a cooling trend for the whole Northern  
328 Hemisphere of  $-0.58 \pm 0.17$  °C/decade in NCEP,  $-0.30 \pm 0.16$  °C/decade in RICH and  $-0.48 \pm 0.20$   
329 °C/decade in FU-Berlin. For the common post-1980s period (1980-2001), the respective  
330 trends are  $-0.79 \pm 0.18$  °C/decade in NCEP,  $-0.66 \pm 0.16$  °C/decade for RICH and  $-0.82 \pm 0.19$   
331 °C/decade in FU-Berlin. The CESM1-WACCM model results agree with re-analysis and the  
332 observations, indicating a persistent cooling of the lower stratosphere during summer for the  
333 whole Northern Hemisphere by  $-0.33 \pm 0.17$  °C/decade for 1958-1979 and by  $-0.35 \pm 0.20$   
334 °C/decade for 1980-2001. However the modelled trends are generally lower than re-analysis  
335 and observations. We should point out that our analysis was also performed for the ERA-40  
336 dataset (not shown here) with the trend results for the two periods (1958-1979 and 1980-  
337 2001) being similar to NCEP trend results.

338 The summertime lower stratosphere trends at the different latitudinal belts (see Table 1 and  
339 Tables SMT1 and SMT2 in supplementary material) indicate generally statistically significant  
340 (at 95%) cooling trends over both pre-1980s and post-1980s periods in the tropics ( $5^{\circ}\text{N}$ - $30^{\circ}\text{N}$ )  
341 and mid-latitudes ( $30^{\circ}\text{N}$  –  $60^{\circ}\text{N}$ ) based on NCEP, FU-Berlin and RICH datasets which is also  
342 reproduced by CESM1-WACCM (Table 2). However, in polar regions ( $60^{\circ}\text{N}$ - $90^{\circ}\text{N}$ ), the  
343 lower stratosphere cooling trends are either non-statistically significant or marginally  
344 significant at the 95% confidence level for NCEP, FU-Berlin and RICH datasets. The same  
345 result is also indicated in CESM1-WACCM simulation (Table 2).

346 In the lower northern hemispheric troposphere (1000-500 hPa), non-statistically significant (at  
347 95%) trends or slight cooling trends prevail in the period 1958-1979 ( $0.06 \pm 0.06$  for NCEP and  
348  $-0.12 \pm 0.06$  °C/decade for RICH) followed by significant warming trends over the period  
349 1980-2005 ( $0.25 \pm 0.05$  °C/decade for both NCEP and RICH). CESM1-WACCM shows a  
350 persistent warming of the lower troposphere during summer by  $0.21 \pm 0.17$  °C/decade in the  
351 pre-1980s period and  $0.21 \pm 0.14$  °C/decade in the post-80s period. However, when excluding

352 the polar latitudes, CESM1-WACCM shows a non-statistically significant (at 95%) trend in  
353 the period 1958-1979 ( $0.04\pm 0.12$  °C/decade) followed by a warming trend over the period  
354 1980-2005 ( $0.22\pm 0.11$  °C/decade) in agreement with NCEP and RICH.

355 The NCEP tropopause pressure follows closely (but in reverse) the tropospheric temperature  
356 long term change with tropopause pressure increasing in the pre-1980s period (tropopause  
357 height decreases) and decreasing in the post-80s period (tropopause height increases) at all  
358 three latitude zones. It should be pointed out that the increasing trend of tropopause pressure  
359 over the tropics in the pre-80s period is small and not statistically significant at 95% level.  
360 The summer CESM1-WACCM tropopause pressure trends (Table 2) generally agree within 1-  
361 sigma with the respective NCEP trends (Table 1) with exception for the mid-latitudes of the  
362 pre-1980s period where CESM1-WACCM shows a statistical significant decreasing trend  
363 (tropopause height increases).

364 The year-round temperature and tropopause trends (Figure 2) generally show similar results to  
365 those derived for the summer period (see also Tables SMT3, SMT4, SMT5 and SMT6 in the  
366 supplementary material). In the lower stratosphere, the layer mean temperatures are  
367 decreasing continuously from late 1950s and throughout the records onwards. Specifically, for  
368 the period 1958-1979, there is a cooling trend for the whole Northern Hemisphere of -  
369  $0.58\pm 0.08$  °C/decade in NCEP,  $-0.33\pm 0.08$  °C/decade in RICH and  $-0.44\pm 0.10$  °C/decade in  
370 FU-Berlin. For the common for all datasets period 1980-2001, the respective trends are -  
371  $0.76\pm 0.09$  °C/decade in NCEP,  $-0.64\pm 0.08$  °C/decade for RICH and  $-0.71\pm 0.10$  °C/decade in  
372 FU-Berlin. The CESM1-WACCM model shows also a persistent cooling of the lower  
373 stratosphere by  $-0.40\pm 0.09$  °C/decade for 1958-1979 and by  $-0.24\pm 0.10$  °C/decade for 1980-  
374 2001. The decreasing trends of lower stratospheric temperatures are statistically significant (at  
375 95% confidence level) at the tropical belt ( $5^{\circ}\text{N}$ - $30^{\circ}\text{N}$ ) and the mid-latitudes ( $30^{\circ}\text{N}$ - $60^{\circ}\text{N}$ ) for  
376 all datasets. For the polar latitudes ( $60^{\circ}\text{N}$ - $90^{\circ}\text{N}$ ), it should be noted the non-statistically  
377 significant (95%) small negative temperature (or even positive) trend during the pre-1980s  
378 period at the lower stratosphere in both RICH and FU-Berlin datasets in contrast to NCEP and  
379 CESM1-WACCM. For the post-1980s period in the lower stratosphere over polar latitudes all  
380 datasets indicate statistically significant cooling trends but with the tension in CESM1-  
381 WACCM simulation for a smaller cooling trend.

382 In the lower troposphere over the Northern Hemisphere, an insignificant change or a small  
383 cooling trend from the beginning of our datasets through the end of 1970s, ( $0.01\pm 0.03$  for  
384 NCEP and  $-0.13\pm 0.03$  °C/decade for RICH) is followed by a statistically significant warming

385 trend in the post-1980s period ( $0.30\pm 0.02$  for NCEP and  $0.27\pm 0.02$  °C/decade for RICH).  
386 CESM1-WACCM shows a persistent warming of the lower troposphere during summer by  
387  $0.23\pm 0.09$  °C/decade in the pre-1980s period and  $0.28\pm 0.07$  °C/decade in the post-80s period.  
388 Tropospheric temperature trends in CESM1-WACCM simulations (see supplementary  
389 material SMT6) generally agree within 1-sigma with NCEP temperature trends before and  
390 after the 1980s with exception the pre-1980s trend in polar latitudes showing a statistical  
391 significant warming in contrast to NCEP and RICH datasets. When excluding the polar  
392 latitudes, CESM1-WACCM shows a non-statistically significant (at 95%) trend in the period  
393 1958-1979 ( $0.05\pm 0.06$ ) followed by a warming trend over the period 1980-2005 ( $0.24\pm 0.06$   
394 °C/decade) in agreement with NCEP and RICH. It should be noted that the year-round  
395 tropospheric temperature trends in the post-1980s period calculated in NCEP (see  
396 supplementary material SMT3), RICH (see supplementary material SMT4) and WACCM  
397 model (see supplementary material SMT6) for the three latitudinal belts are within the range  
398 of respective calculations in previously published work based on different radiosonde datasets  
399 (Randel et al., 2009).

400 The effects of natural forcings derived from our multi-linear regression analysis are in  
401 generally good agreement with previous studies (e.g. Randel et al., 2009), given that we use  
402 layer-mean temperatures and different latitude band averages. The effects of solar and  
403 volcanic forcing are found to be more pronounced after 1980. Although the QBO signal is  
404 very small and insignificant in the troposphere, we have used the same regression model  
405 throughout the atmosphere for uniformity and consistency.

406

407

### 408 **3.2 Monthly trends**

409 The temperature trends were also calculated on a monthly basis. The layer mean temperature  
410 trends based on NCEP reanalysis (Figure 3) are persistently negative at the lower stratosphere  
411 for all months, for both periods before and after 1979 at the tropical and mid-latitude  
412 latitudinal belts. The monthly temperature trends based on the RICH dataset (Figure 4) and  
413 the FU-Berlin dataset (Figure 5) also show persistent negative temperature trends in the lower  
414 stratosphere for all months for both periods before and after 1979 at the tropical and mid-  
415 latitude latitudinal belts, in agreement with NCEP. The CESM1-WACCM simulation  
416 reproduces the cooling trends in the lower stratosphere for both pre-1980s and post-1980s at  
417 the tropical and mid-latitude latitudinal belts (Figure 6).

418 At polar latitudes, we find non-statistically significant (at 90% confidence level) cooling  
419 trends for all months in NCEP, except in February-March with a characteristic abrupt  
420 enhancement of the cooling trend for the pre-1980s (Fig. 3e). In the post-80s period the  
421 cooling trends are non-statistically significant for all months except in March-April with  
422 strongest cooling signal which might be associated to the Arctic ozone depletion by ODSs  
423 (Figure 3f). In the lower stratosphere over polar latitudes for the pre-1980s period, both RICH  
424 (Figure 4e) and FU-Berlin (Figures 5a and 5c) datasets do not show statistically significant (at  
425 90% confidence level) negative trends. However, it should be noted that the abrupt shift in  
426 trend from winter to early spring is a common feature in all three datasets which could be  
427 related to dynamical processes and the related variability of the polar vortex. In the post-  
428 1980s period both RICH and FU-Berlin datasets indicate cooling trends maximizing in early  
429 spring in agreement with the NCEP results presumably due to the ozone depletion issue  
430 within the Arctic polar vortex. The CESM1-WACCM simulation captures at polar latitudes  
431 (Figure 6e) the abrupt decrease (or elimination) of the cooling trend from winter to early  
432 spring for the pre-1980s period but the winter cooling trends are much stronger than in NCEP,  
433 RICH and FU-Berlin datasets. In the post-1980s period the cooling trends are non-statistically  
434 significant (at 90% confidence level) for all months and the early-spring cooling trend seen in  
435 NCEP, RICH and FU-Berlin datasets (due to ODSs) is not captured or is smaller (Figure 6f).  
436 Overall, all datasets indicate that persistent cooling trends in the lower stratosphere exist in all  
437 months and for both periods before and after 1979 which is a robust feature over the tropical  
438 belt and the middle latitudes.

439

### 440 **3.3 Tropopause - Temperature correlation**

441 As seen in Figures 1 and 2, the tropopause pressure follows closely (but reversed) the  
442 tropospheric temperature long-term course with a cooling trend or absence of a trend until  
443 about the end of the 1970s and a warming trend from about the mid-1980s until present.  
444 Moving up in the lower stratosphere, we have seen that all datasets show persistent cooling  
445 temperature trends for both the pre-1980s and post-1980s periods (Figure 1 and Figure 2). In  
446 this section we investigate the interannual correlation of temperature with tropopause pressure  
447 on a monthly basis with the aim of unraveling the relative contribution of tropospheric and  
448 stratospheric temperatures on the interannual and long-term variability of tropopause  
449 pressure. As has been pointed out in previous studies, the interannual variability and the  
450 trends in tropopause height are mainly determined by the interannual variability and the

451 trends of temperature in the lower stratosphere and upper troposphere (Seidel et al., 2006; Son  
452 et al., 2009).

453 At the tropical latitudinal belt (5N-30N) the pearson correlation between tropopause pressure  
454 and layer mean temperature (based on NCEP reanalysis) is negative in the troposphere  
455 ranging from -0.3 to -0.7 becoming positive and stronger in the lower stratosphere ranging  
456 from 0.6 to 0.9 (Figure 7a). The negative correlations in the troposphere have a seasonal  
457 signal with the tendency to get stronger during the summer period while in the lower  
458 stratosphere the strong positive correlation persists throughout the course of the year. Hence it  
459 is inferred from Figure 7a that throughout the year the interannual variance of the lower  
460 stratospheric temperatures contribute to the interannual variability at the tropopause region, a  
461 higher percentage than that contributed from the variance of tropospheric temperatures. The  
462 relative contribution of tropospheric temperatures in the interannual variance at tropopause  
463 maximizes during the warm period of the year. CESM1-WACCM (Figure 7d) reproduces  
464 fairly well the correlation pattern of NCEP at the tropical band, thus indicating good skill of  
465 the model to simulate the relation in the interannual variability between tropopause height and  
466 temperature in the lower stratosphere/upper troposphere region.

467 At mid-latitudes, the tropopause-temperature correlations in NCEP dataset become weaker,  
468 reaching 0.4 in the lower stratosphere and -0.5 in the troposphere mainly from June to  
469 September (Figure 7b) indicating a higher sensitivity of tropopause interannual changes to  
470 tropospheric temperature changes during the warm season. CESM1-WACCM (Figure 7e)  
471 captures the basic pattern of the tropopause-temperature correlations seen in NCEP for mid-  
472 latitudes.

473 At polar latitudes (60N-90N), the negative correlations (in NCEP) in the troposphere have a  
474 seasonal signal with the tendency to get stronger during the warm period of the year reaching  
475 a value of -0.7 while in the lower stratosphere the positive correlations become stronger  
476 during the cold part of the year reaching a value of 0.8 (Figure 7c). Thus the interannual  
477 variability of lower stratospheric temperature dominates over tropospheric temperature for  
478 controlling the interannual variability of the tropopause during the cold part of the year linked  
479 with the development of the polar vortex. In contrast during the warm period of the year, the  
480 interannual variability of tropospheric temperature takes over stratospheric temperature,  
481 linked to the higher heating rates of the polar troposphere.

482 The tropopause-temperature correlations pattern in CESM1-WACCM over the polar latitudes  
483 (Figure 7f) is similar to the pattern of mid-latitudes and does not capture the NCEP correlation

484 pattern of polar latitudes. A common feature for the three latitudinal belts and for both NCEP  
485 and WACCM is that the negative correlations in the troposphere have a seasonal signal with  
486 the tendency to get stronger during the warm part of the year, linked to the more efficient  
487 mechanism of tropospheric heating to affect the interannual variability of climate variables at  
488 the tropopause region.

489

#### 490 **4 Discussion and concluding remarks**

491 We presented the stratospheric temperature trends from the late 1950s using the  
492 independently produced FU-Berlin stratospheric dataset comprising monthly layer-mean  
493 temperatures derived from geopotential heights together with other analysis using reanalysis  
494 and radiosonde data over the northern hemisphere. After removing the natural variability with  
495 the use of climatic and dynamical indices in a statistical autoregressive multiple regression  
496 model, the calculated year-round trends showed a persistent decrease in temperatures in the  
497 lower stratosphere since the late 50s. This is also confirmed by applying the interannual trend  
498 analyses separately for the summer when the stratosphere is less disturbed, the Brewer-  
499 Dobson circulation is weaker and it is also not influenced at high latitudes by the chemical  
500 ozone depletion due to ODSs found in the winter-early spring period (e.g. Harris et al., 2008).  
501 These decreasing lower stratosphere trends are robust features for NCEP, FU-Berlin and  
502 RICH datasets in the tropics and the middle latitudes. The CESM1-WACCM simulation  
503 reproduces the lower stratosphere cooling trends before and after the 1980s in the tropics and  
504 over mid-latitudes, consistent with an increased infrared emission by CO<sub>2</sub> (Marsh et al.,  
505 2013). It should be noted that modelled trends in the lower stratosphere were found to be  
506 generally lower than those found in the re-analysis and the observations. This result is in  
507 agreement with the study by Santer et al. (2013) who showed that on average the CMIP5  
508 models analysed underestimate the observed cooling of the lower stratosphere maybe due to  
509 the need for a more realistic treatment of stratospheric ozone depletion and volcanic aerosol  
510 forcing.

511 It should be pointed out that the temperature long-term trends based on RICH are within 1-  
512 sigma of the thickness calculated layer temperature trends from FU-Berlin and NCEP datasets  
513 indicating a consistent picture for the cooling trend of the lower stratosphere before and after  
514 the 1980s. The consistency of RICH temperature trends with the thickness calculated layer  
515 mean temperature trends from FU-Berlin and NCEP, enhances our confidence for the cooling  
516 trend in the lower stratosphere in the pre-satellite era despite the documented trend

517 uncertainties of the radiosonde datasets during this period (Randel and Wu, 2006; Free and  
518 Seidel, 2007; Randel et al. 2009). Furthermore the inspection of lower stratospheric trends on  
519 a monthly basis for all datasets indicate the persistent cooling trends in the lower stratosphere  
520 to be a common feature for all months before and after 1980s both at the tropical belt and over  
521 the middle latitudes.

522 The post-1980s lower stratosphere cooling is a common finding in the global mean based on  
523 all available satellite and radiosonde datasets while the stratosphere cooling is also reported  
524 for the pre-satellite era since 1958 (WMO, 2011; Zerefos and Mantis, 1977). Our post-1980  
525 year round stratospheric temperature trends at layers L4 (100-50 hPa) and L5 (50-30 hPa) are  
526 in the range of calculated trends in Microwave Sounding Unit (MSU) channel 4 (15-20 km)  
527 and Stratospheric Sounding Unit (SSU) channel 1 (25-35 km). MSU channel 4 trends derived  
528 from RSS and UAH data show cooling trends over the Northern Hemisphere ranging from -  
529 0.2 °C/decade to -0.5 °C/decade over the period 1979-2007 (Randel et al., 2009). Comparable  
530 cooling trends were obtained for MSU channel 4 after reprocessing by NOAA with the trends  
531 at polar latitudes revealing higher uncertainties. The SSU channel 1 trends as processed by the  
532 UK Met Office and reprocessed by NOAA show cooling trends ranging from about -0.5  
533 °C/decade (Met office) to about -1.1 °C/decade (NOAA) over the period 1979-2005  
534 (Thompson et al., 2012).

535 These long term cooling trends in the lower stratosphere can be maintained by increasing  
536 GHGs that cool the stratosphere while warming the troposphere (IPCC, 2007 and references  
537 therein; Polvani and Solomon, 2012). The post 1980s decrease in stratospheric ozone in late  
538 winter-early spring at mid and polar latitudes of Northern Hemisphere due to ODSs  
539 complicates the issue (Harris et al., 2008). However the persistence of the cooling trends in  
540 the lower stratosphere for all months and especially during the less disturbed summer period  
541 with the reduced interannual variance which are observed both before and after the 1980s  
542 over the tropics and the mid-latitudes indicates that the anthropogenic enhanced greenhouse  
543 effect is the most plausible cause for the observed stratospheric quasi monotonous cooling in  
544 the Northern Hemisphere.

545 At polar latitudes (60°N-90°N) the cooling trends in the lower stratosphere are either non-  
546 statistically significant or marginally significant at the 95% confidence level for all datasets.  
547 This finding could be related to the competing dynamical and radiative processes that reduce  
548 the statistical significance of these trends. A number of modeling studies suggest that the  
549 greenhouse warming leads to stronger tropical upwelling and stronger Brewer-Dobson (BD)

550 circulation (Rind et al., 2001; Cordero and Forster, 2006; Butchart et al., 2006; Butchart et al.,  
551 2010; Austin and Li, 2006; Rosenlof and Reid, 2008; Garcia and Randel, 2008; Lamarque and  
552 Solomon, 2010). The GHG induced strengthening of BD circulation may lead to a relatively  
553 warmer lower stratosphere at higher latitudes thus masking the GHGs radiatively cooling  
554 discussed before. In contrast, over the tropics both dynamical and radiative processes act  
555 towards the same direction i.e. the cooling in the lower stratosphere. Our results are in line  
556 with other recent studies. For example, Thompson and Solomon (2009) demonstrated that the  
557 contrasting latitudinal structures of recent stratospheric temperature (i.e., stronger cooling in  
558 the tropical lower stratosphere than in the extratropics) and ozone trends (i.e., enhanced ozone  
559 reduction in the tropical lower stratosphere) are consistent with the assumption of increases in  
560 the stratospheric overturning BD circulation. Free (2011) also pointed that the trends in the  
561 tropical stratosphere show an inverse relationship with those in the Arctic for 1979–2009,  
562 which might be related to changes in stratospheric circulation.

563 In the troposphere, a common feature in the RICH and NCEP datasets is a non-statistically  
564 significant trend or a slight cooling trend until about the end of the 1970s, followed by a  
565 warming trend until the present day for the three latitudinal belts. This pre-1980s cooling  
566 trend (or absence of trend) in the troposphere is associated with a notable cooling trend from  
567 the late 1940s to 1970s (IPCC, 2007), which has been raised as a point of weakness against  
568 the advocates of the theory of CO<sub>2</sub> related anthropogenic global warming (Thompson et al.,  
569 2010). However, apart from the important role of the decadal natural variability hampering  
570 the anthropogenic climate change (Ring et al., 2012; Kosaka and Xie, 2013), anthropogenic  
571 aerosols also attracted the scientific interest as a possible cause for this mid-century cooling  
572 due to a high concentration of sulfate aerosols emitted in the atmosphere by industrial  
573 activities and volcanic eruptions during this period causing the so-called “solar dimming”  
574 effect (e.g. Wild et al., 2007; Zerefos et al., 2012). Hence the pre-1980s small cooling trend or  
575 insignificant change might be due to natural variability in the ocean-atmosphere system in  
576 combination with the compensating role of anthropogenic aerosols in the troposphere.  
577 Concerns have been raised recently that increases in aerosol from anthropogenic air pollution  
578 and associated dimming of surface solar radiation could have masked to a large extent the  
579 temperature rise induced by increasing greenhouse gases, so that the observed temperature  
580 records would not reflect the entire dimension of greenhouse warming (Andreae et al., 2005;  
581 Wild et al., 2007).

582 The investigation of the interannual correlation of tropopause pressure with tropospheric and

583 stratospheric temperatures showed a few distinct characteristics. A common feature for the  
584 three latitudinal belts in both NCEP and CESM1-WACCM is that the influence of  
585 tropospheric temperature on the interannual variability of tropopause has a seasonal signal  
586 with the tendency to get stronger during the warm period of the year when the tropospheric  
587 heating maximizes.

588 In the tropics ( $5^{\circ}\text{N}$ - $30^{\circ}\text{N}$ ), the interannual variability of lower stratospheric temperature  
589 dominates over tropospheric temperature for controlling the interannual variability of the  
590 tropopause throughout the year in both NCEP and CESM1-WACCM. This could possibly  
591 explain why at the tropical zone ( $5^{\circ}\text{N}$ - $30^{\circ}\text{N}$ ) there is a decreasing trend of tropopause pressure  
592 (increase of tropopause height) in the pre-1980s. Seidel and Radel (2006) also reported using  
593 radiosonde data that on the multidecadal scale for tropical atmosphere, the tropopause height  
594 change is more sensitive to stratospheric temperature change than tropospheric change and  
595 hence at the lowest frequencies the tropopause is primarily coupled with stratospheric  
596 temperatures.

597 At mid-latitudes the tropopause pressure - temperature correlations become generally weaker  
598 maximizing from June to September with tropospheric temperatures slightly overwhelming  
599 stratospheric temperatures for the control of the interannual variability of tropopause. This is  
600 in line with the study of Son et al. (2009) who analysed a set of long-term integrations with  
601 stratosphere-resolving chemistry climate models (CCMs) and reported that at mid-latitudes  
602 the linear tropopause height increase is rather controlled by the upper troposphere warming  
603 rather than the lower stratosphere cooling. Wu et al. (2013) reported a significant positive  
604 correlation between the changes in the tropospheric temperature induced by aerosols and  
605 tropopause height at mid-latitudes, the zone between  $30^{\circ}$  and  $60^{\circ}$  in both hemispheres. Hence  
606 taking into account the anthropogenic aerosols variability in the troposphere, the tropopause  
607 trends at mid-latitudes may not solely reflect human induced climate change signal from  
608 GHGs.

609 At polar latitudes (in NCEP) the interannual variability of lower stratospheric temperature  
610 dominates over tropospheric temperature for controlling the interannual variability of the  
611 tropopause during the cold part of the year (linked with the development of the polar vortex)  
612 while the opposite occurs during the warm period of the year (linked to the higher heating  
613 rates of polar troposphere). However, during the late winter-early spring, chemical ozone  
614 depletion within polar Arctic stratosphere in the post-1980s period could further cool the  
615 lower stratosphere (in addition to the radiative effect of GHGs) leading possibly to an even

616 higher tropopause. The GHGs induced strengthening of BD circulation, which leads to a  
617 relatively warmer lower stratosphere (thus masking the GHGs radiatively cooling) and lower  
618 tropopause, further complicates the issue of using lower stratosphere temperature and  
619 tropopause height as climate change indicators at polar latitudes. CESM1-WACCM at polar  
620 latitudes does not capture the respective NCEP correlation pattern, an issue that needs further  
621 investigation.

622 The relative contribution of lower stratosphere versus troposphere for the control of  
623 tropopause low frequency variability is an important issue for understanding past and future  
624 tropopause trends in view also of the monotonically increasing future tropopause height  
625 trends till the end of 21st century predicted by both stratosphere-resolving chemistry climate  
626 models (CCMs) and the Intergovernmental Panel on Climate Change Fourth Assessment  
627 Report (AR4) models (Son et al., 2009).

628 In conclusion, we provide additional evidence for an early greenhouse cooling signal of the  
629 lower stratosphere before the 1980s, which appears earlier than the tropospheric greenhouse  
630 warming signal. As a result, it may be that the stratosphere could have provided an early  
631 warning of human-produced climate change. In line with the theoretical expectations that  
632 equilibrium temperature in the stratosphere compared to the troposphere is more sensitive to  
633 anthropogenic GHGs and less sensitive to tropospheric water vapour, aerosols and clouds, it is  
634 tentatively proposed that the stratosphere is more suitable for the detection of man-made  
635 climate change signal. We suggest that the maintenance and enrichment of the ground-based  
636 and satellite global networks for monitoring stratospheric temperatures and the tropopause  
637 region, which adds value in understanding the behaviour of the interface between the  
638 troposphere and stratosphere, are essential steps to unravel the issue of future human induced  
639 climate change signals.

640

## 641 **Acknowledgments**

642 For University of Illinois, this research was supported in part from NASA under project  
643 NASA NNX12AF32G. We acknowledge the support provided by the Mariolopoulos-  
644 Kanaginis Foundation for the Environmental Sciences. Prodromos Zanis and Juerg  
645 Luterbacher would like also to acknowledge the support in the framework of the Greece-  
646 Germany Exchange and Cooperation Programme, IKYDA 2012. The FU-Berlin dataset was  
647 obtained by K. Labitzke and Collaborators, 2002: The Berlin Stratospheric Data Series, CD  
648 from the Meteorological Institute, Free University Berlin. NCEP Reanalysis derived data

649 provided by the NOAA/OAR/ESRL PSD, Boulder, Colorado, USA, from their Web site at  
650 <http://www.cdc.noaa.gov/>. The authors would like to thank the anonymous reviewers for their  
651 valuable comments and suggestions.

652

653

654 **References**

- 655 Andreae, M. O., Jones, C. D., and Cox, P. M.: Strong present-day aerosol cooling implies a  
656 hot future, *Nature*, 435, 1187–1190, doi:10.1038/nature03671, 2005.
- 657 Angell, J. K. and Korshover J.: Global temperature variations in the troposphere and  
658 stratosphere, 1958-1982, *Mon. Weather Rev.*, 111, 901-921, 1983.
- 659 Austin, J. and Li, F.: On the relationship between the strength of the Brewer-Dobson  
660 circulation and the age of stratospheric air, *Geophys. Res. Lett.*, 33, L17807,  
661 doi:10.1029/2006GL026867, 2006.
- 662 Austin, J., Wilson, R. J., Akiyoshi, H., Bekki, S., Butchart, N., Claud, C., Fomichev, V. I.,  
663 Forster, P., Garcia, R. R., Gillett, N. P., Keckhut, P., Langematz, U., Manzini, E.,  
664 Nagashima, T., Randel, W. J., Rozanov, E., Shibata, K., Shine, K. P., Struthers, H.,  
665 Thompson, D. W. J., Wu, F., and Yoden, S.: Coupled chemistry climate model  
666 simulations of stratospheric temperatures and their trends for the recent past, *Geophys.*  
667 *Res. Lett.*, 36, L13809, doi:10.1029/2009GL038462, 2009.
- 668 Berger, U., and F.-J. Lübken (2011), Mesospheric temperature trends at midlatitudes in  
669 summer, *Geophys. Res. Lett.*, 38, L22804, doi:10.1029/2011GL049528.
- 670 Butchart, N., Scaife, A. A., Bourqui, M., de Grandpré, J., Hare, S. H. E., Kettleborough, J.,  
671 Langematz, U., Manzini, E., Sassi, F., Shibata, K., Shindell, D., and Sigmond, M.:  
672 Simulations of anthropogenic change in the strength of the Brewer–Dobson circulation,  
673 *Clim. Dyn.*, 27, 727–741, doi:10.1007/s00382-006-0162-4, 2006.
- 674 Butchart, N., Cionni, I., Eyring, V., Shepherd, T. G., Waugh, D. W., Akiyoshi, H., Austin, J.,  
675 Brühl, C., Chipperfield, M. P., Cordero, E., Dameris, M., Deckert, R., Dhomse, S., Frith,  
676 S. M., Garcia, R. R., Gettelman, A., Giorgetta, M. A., Kinnison, D. E., Li, F., Mancini, E.,  
677 McLandress, C., Pawson, S., Pitari, G., Plummer, D. A., Rozanov, E., Sassi, F., Scinocca,  
678 J. F., Shibata, K., Steil, B., and Tian, W.: Chemistry-climate model simulations of twenty-  
679 first century stratospheric climate and circulation change, *J. Climate.*, 23, 5349–5374,  
680 doi:10.1175/2010JCLI3404.1, 2010.
- 681 Butchart, N.: The Brewer-Dobson Circulation, *Reviews of Geophysics*, doi:  
682 10.1002/2013RG000448, 2014.
- 683 Christy, J. R., Spencer, R. W., Norris, W. B., Braswell, W. D., and Parker, D. E.: Error  
684 estimates of version 5.0 of MSU-AMSU bulk atmospheric temperatures, *J. Atmos.*

- 685 Oceanic Technol., 20, 613-629, 2003.
- 686 Cordero, E. and Forster, P.: Stratospheric variability and trends in models used for the IPCC  
687 AR4, Atmos. Chem. Phys., 6, 5369–5380, doi:10.5194/acp-6-5369-2006, 2006.
- 688 Crooks, S. A. and Gray, L. J.: Characterization of the 11-year solar signal using a multiple  
689 regression analysis of the ERA-40 dataset, J. Climate, 18, 996–1015, 2005.
- 690 Engel, A., Möbius, T., Bönisch, H., Schmidt, U., Heinz, R., Levin, I., Atlas, E., Aoki, S.,  
691 Nakazawa, T., Sugawara, S., Moore, F., Hurst, D., Elkins, J., Schauffler, S., Andrews, A.,  
692 and Boering, K.: Age of stratospheric air unchanged within uncertainties over the past 30  
693 years, Nature Geoscience, 2, 28–31, doi:10.1038/ngeo388, 2009.
- 694 Free, M.: The Seasonal Structure of Temperature Trends in the Tropical Lower Stratosphere,  
695 J. Climate, 24, 859–866, doi:10.1175/2010JCLI3841.1, 2011.
- 696 Free, M. and Lanzante, J.: Effect of volcanic eruptions on the vertical temperature profile in  
697 radiosonde data and climate models, J. Climate, 22, 2925-2939,  
698 doi:10.1175/2008JCLI2562.1, 2009.
- 699 Free, M. and Seidel D. J.: Comments on “Biases in Stratospheric and Tropospheric  
700 Temperature Trends Derived from Historical Radiosonde Data”, J. Climate, 20, 3704-  
701 3709, doi:10.1175/JCLI4210.1, 2007.
- 702 Free, M., Seidel, D. J., Angell, J. K., Lanzante, J., Durre, I., and Peterson, T. C.: Radiosonde  
703 Atmospheric Temperature Products for Assessing Climate (RATPAC): A new data set of  
704 large-area anomaly time series, J. Geophys. Res., 110, D22101,  
705 doi:10.1029/2005JD006169, 2005.
- 706 Fioletov, V. E.: Estimating the 27-day and 11-year solar cycle variations in tropical upper  
707 stratospheric ozone, J. Geophys. Res., 114, D02302, doi:10.1029/2008JD010499, 2009.
- 708 Fu, Q., Solomon, S., and Lin, P.: On the seasonal dependence of tropical lower-stratospheric  
709 temperature trends, Atmos. Chem. Phys., 10, 2643–2653, 2010.
- 710 Garcia, R. R. and Randel, W. J.: Acceleration of the Brewer-Dobson circulation due to  
711 increases in greenhouse gases, J. Atmos. Sci., 65, 2731–2739,  
712 doi:10.1175/2008JAS2712.1, 2008.
- 713 Gettelman, A., Hoor, P., Pan, L. L., Randel, W. J., Hegglin, M. I., and Birner, T.: The  
714 extratropical upper troposphere and lower stratosphere, Rev. Geophys., 49, RG3003,  
715 doi:10.1029/2011RG000355, 2011.

- 716 Haimberger, L.: Homogenization of radiosonde temperature time series using innovation  
717 statistics, *J. Climate*, 20, 1377-1403, doi:10.1175/JCLI4050.1, 2007.
- 718 Haimberger, L., Tavolato, C., and Sperka, S.: Toward elimination of the warm bias in historic  
719 radiosonde temperature records—Some new results from a comprehensive  
720 intercomparison of upper-air data, *J. Climate*, 21, 4587–4606,  
721 doi:10.1175/2008JCLI1929.1, 2008.
- 722 Harris, N. R. P., Kyrö, E., Staehelin, J., Brunner, D., Andersen, S.-B., Godin-Beekmann, S.,  
723 Dhomse, S., Hadjinicolaou, P., Hansen, G., Isaksen, I., Jrrar, A., Karpetchko, A., Kivi, R.,  
724 Knudsen, B., Krizan, P., Lastovicka, J., Maeder, J., Orsolini, Y., Pyle, J. A., Rex, M.,  
725 Vanicek, K., Weber, M., Wohltmann, I., Zanis, P., and Zerefos, C.: Ozone trends at  
726 northern mid- and high latitudes – a European perspective, *Ann. Geophys.*, 26, 1207–  
727 1220, 2008.
- 728 He, Q., Li, C., Mao, J., Lau, A. K.-H., and Chu, D. A.: Analysis of aerosol vertical distribution  
729 and variability in Hong Kong, *J. Geophys. Res.*, 113, D14211,  
730 doi:10.1029/2008JD009778, 2008.
- 731 Holland, M. M., Bailey, D. A., Briegleb, B. P., Light, B., and Hunke, E.: Improved Sea Ice  
732 Shortwave Radiation Physics in CCSM4: The Impact of Melt Ponds and Aerosols on  
733 Arctic Sea Ice, *J. Climate*, 25, 1413–1430, doi:10.1175/JCLI-D-11-00078.1, 2012.
- 734 Hu, Y. and Fu, Q.: Stratospheric warming in Southern Hemisphere high latitudes since 1979,  
735 *Atmos. Chem. Phys.*, 9, 4329–4340, doi:10.5194/acp-9-4329-2009, 2009.
- 736 IPCC, *Climate Change 2007: The Physical Science Basis. Contribution of Working Group I to*  
737 *the Fourth Assessment, Report of the Intergovernmental Panel on Climate Change*  
738 *[Solomon, S., Qin, D., Manning, M., Chen, Z., Marquis, M., Averyt, K. B., Tignor M.,*  
739 *and Miller, H. L. (Eds.)]. Cambridge University Press, Cambridge, United Kingdom and*  
740 *New York, NY, USA, 996 pp., 2007.*
- 741 IPCC, *Climate Change 2013: The Physical Science Basis. Contribution of Working Group I to*  
742 *the Fifth Assessment Report (AR5) of the Intergovernmental Panel on Climate,*  
743 <http://www.climatechange2013.org/>, 2013.
- 744 Iwasaki, T., Hamada, H., and Miyazaki, K.: Comparisons of Brewer-Dobson circulations  
745 diagnosed from reanalyses, *J. Meteorol. Soc. Jpn.*, 87, 997–1006,  
746 doi:10.2151/jmsj.87.997, 2009.

- 747 Johanson, C. M. and Fu, Q.: Antarctic atmospheric temperature trend patterns from satellite  
748 observations, *Geophys. Res. Lett.*, 34, L12703, doi:10.1029/2006GL029108, 2007.
- 749 Kalnay, E., Kanamitsu, M., Kistler, R., Collins, W., Deaven, D., Gandin, L., Iredell, M., Saha,  
750 S., White, G., Woollen, J., Zhu, Y., Leetmaa, A., Reynolds, R., Chelliah, M., Ebisuzaki,  
751 W., Higgins, W., Janowiak, J., Mo, K. C., Ropelewski, C., Wang, J., Jenne, R., and  
752 Joseph, D.: The NCEP/NCAR 40-Year Reanalysis Project, *Bull. Amer. Meteor. Soc.*, 77,  
753 437–471, 1996.
- 754 Kawatani, Y. and Hamilton, K.: Weakened stratospheric quasibiennial oscillation driven by  
755 increased tropical mean upwelling, *Nature*, 497, 478–481, doi:10.1038/nature12140,  
756 2013.
- 757 Kinnison, D. E., Brasseur, G. P., Walters, S., Garcia, R. R., Marsh, D. R., Sassi, F., Harvey, V.  
758 L., Randall, C. E., Emmons, L., Lamarque, J. F., Hess, P., Orlando, J. J., Tie, X. X.,  
759 Randel, W., Pan, L. L., Gettelman, A., Granier, C., Diehl, T., Niemeier, U., and Simmons,  
760 A. J.: Sensitivity of chemical tracers to meteorological parameters in the MOZART-3  
761 chemical transport model, *J. Geophys. Res.*, 112, D20302, doi:10.1029/2006JD007879,  
762 2007.
- 763 Kistler, R., Kalnay, E., Collins, W., Saha, S., White, G., Woollen, J., Chelliah, M., Ebisuzaki,  
764 W., Kanamitsu, M., Kousky, V., van den Dool, H., Jenne, R., and Fiorino, M.: The NCEP-  
765 NCAR 50-Year Reanalysis: Monthly Means CD-ROM and Documentation, *Bull. Amer.*  
766 *Meteor. Soc.*, 82, 247–267, 2001.
- 767 Kosaka, Y., and Xie, S.P.: Recent global-warming hiatus tied to equatorial Pacific surface  
768 cooling, *Nature*, doi:10.1038/nature12534, 2013.
- 769 Labitzke, K., and Coauthors: The Berlin Stratospheric Data Series. Meteorological Institute,  
770 Free University Berlin, CD-ROM, 2002.
- 771 Labitzke, K. and Kunze, M.: Stratospheric temperatures over the Arctic: Comparison of three  
772 data sets, *Meteorologische Zeitschrift*, 14(1), 65-74, 2005.
- 773 Lamarque, J.-F. and Solomon S.: Impact of changes in climate and halocarbons on recent  
774 lower stratospheric ozone and temperature trends, *J. Climate*, 23, 2599–2611,  
775 doi:10.1175/2010JCLI3179.1, 2010.
- 776 Lin, P., Fu, Q., Solomon, S., and Wallace, J. M.: Temperature trend patterns in Southern  
777 Hemisphere high latitudes: novel indicators of stratospheric changes, *J. Climate*, 22,

- 778 6325–6341, doi:10.1175/2009JCLI2971.1, 2009.
- 779 Manabe, S. and Weatherald, R. T.: Thermal equilibrium of the atmosphere with a given  
780 distribution of relative humidity, *J. Atmos. Sci.*, 24, 241–259, 1967.
- 781 Manney, G. L., Krüger, K., Sabutis, J. L., Sena, S. A., and Pawson, S.: The remarkable 2003–  
782 2004 winter and other recent warm winters in the Arctic stratosphere since the late 1990s,  
783 *J. Geophys. Res.*, 110, D04107, doi:10.1029/2004JD005367, 2005.
- 784 Marsh, D. R., Mills, M. J., Kinnison, D. E., Lamarque, J.-F., Calvo, N., and Polvani, L. M.:  
785 Climate Change from 1850 to 2005 Simulated in CESM1(WACCM), *J. Climate*, 26,  
786 7372–7391, doi:10.1175/JCLI-D-12-00558.1, 2013.
- 787 Mears, C. A. and Wentz, F. J.: Construction of the Remote Sensing Systems V3.2 atmospheric  
788 temperature records from the MSU and AMSU microwave sounders, *J. Atmos. Oceanic*  
789 *Technol.*, 26, 1040–1056, doi:10.1175/2008JTECHA1176.1, 2009.
- 790 Miller, A. J., Nagatani, R. M., Tiao, G. C., Niu, X. F., Reinsel, G. C., Wuebbles, D., Grant, K.:  
791 Comparisons of observed ozone and temperature trends in the lower stratosphere,  
792 *Geophys. Res. Lett.*, 19, 929–932, 1992.
- 793 Polvani, L. M. and Solomon, S.: The signature of ozone depletion on tropical temperature  
794 trends, as revealed by their seasonal cycle in model integrations with single forcings, *J.*  
795 *Geophys. Res.*, 117, D17102, doi:10.1029/2012JD017719, 2012.
- 796 Randel, W. J. and Wu, F.: Biases in stratospheric and tropospheric temperature trends derived  
797 from historical radiosonde data, *J. Climate*, 19, 2094–2104, 2006.
- 798 Randel, W. J. and Thompson, A. M.: Interannual variability and trends in tropical ozone  
799 derived from SAGE II satellite data and SHADOZ ozonesondes, *J. Geophys. Res.*, 116,  
800 D07303, doi:10.1029/2010JD015195, 2011.
- 801 Randel, W.J., Udelhofen F., Fleming, E., Geller, M., Gelman, M., Hamilton, K., Karoly, D.,  
802 Ortland, D., Pawson, S., Swinbank, R., Wu, F., Baldwin, M., Chanin, M., Keckhut, P.,  
803 Labitzke, K., Remsberg, E., Simmons, A. and Wu, D.: The SPARC intercomparison of  
804 middle-atmosphere climatologies. *Journal of Climate*, 17, 986-1003, 2004.
- 805 Randel, W. J., Shine, K. P., Austin, J., Barnett, J., Claud, C., Gillet, N. P., Keckhut, P.,  
806 Langematz, U., Lin, R., Long, C., Mears, C., Miller, A., Nash, J., Seidel, D. J.,  
807 Thompson, D. W. J., Wu, F., and Yoden, S.: An update of observed stratospheric  
808 temperature trends, *J. Geophys. Res.*, 114, D02107, doi:10.1029/2008JD010421, 2009.

- 809 Ramaswamy, V., Schwarzkopf, M. D., Randel, W. J., Santer, B. D., Soden, B. J., and  
810 Stenchikov, G. L.: Anthropogenic and natural influences in the evolution of lower  
811 stratospheric cooling, *Science*, 311, 1138–1141, doi:10.1126/science.1122587, 2006.
- 812 Reinsel, G. C.: Trend analysis of upper stratospheric Umkehr ozone data for evidence of  
813 turnaround, *Geophys. Res. Lett.*, 29, 1451, doi:10.1029/2002GL014716, 2002.
- 814 Reinsel, G. C., Miller, A. J., Weatherhead, E. C., Flynn, L. E., Nagatani, R. M., Tiao, G. C.,  
815 and Wuebbles D. J.: Trend analysis of total ozone data for turnaround and dynamical  
816 contributions, *J. Geophys. Res.*, 110, D16306, doi:10.1029/2004JD004662, 2005.
- 817 Rind, D., Lerner, J., and McLinden, C.: Changes of tracer distributions in the doubled CO<sub>2</sub>  
818 climate, *J. Geophys. Res.*, 106, 28 061–28 079, doi:10.1029/2001JD000439, 2001.
- 819 Ring M. J., Lindner, D., Cross, E.M., and Schlesinger, M.E.: Causes of the Global Warming  
820 Observed since the 19th Century, *Atmospheric and Climate Sciences*, 2012, 2, 401-415,  
821 doi:10.4236/acs.2012.24035, 2012.
- 822 Rosenlof, K. H. and Reid, G. C.: Trends in the temperature and water vapor content of the  
823 tropical lower stratosphere: Sea surface connection, *J. Geophys. Res.*, 113, D06107,  
824 doi:10.1029/2007JD009109, 2008.
- 825 Santer, B. D., Hnilo, J. J., Wigley, T. M. L., Boyle, J. S., Doutriaux, C., Fiorino, M., Parker, D.  
826 E., and Taylor, K. E.: Uncertainties in observationally based estimates of temperature  
827 change in the free atmosphere, *J. Geophys. Res.*, 104, 6305–6333, doi:  
828 10.1029/1998JD200096, 1999.
- 829 Santer, B. D., Sausen, R., Wigley, T. M. L., Boyle, J. S., AchutaRao, K., Doutriaux, C.,  
830 Hansen, J. E., Meehl, G. A., Roeckner, E., Ruedy, R., Schmidt, G., and Taylor, K. E.:  
831 Behavior of tropopause height and atmospheric temperature in models, reanalyses, and  
832 observations: Decadal changes, *J. Geophys. Res.*, 108, 4002, doi:10.1029/2002JD002258,  
833 2003a.
- 834 Santer, B. D., Wehner, M. F., Wigley, T. M. L., Sausen, R., Meehl, G. A., Taylor, K. E.,  
835 Ammann, C., Arblaster, J., Washington, W. M., Boyle, J. S., and Brüggemann, W.:  
836 Contributions of anthropogenic and natural forcing to recent tropopause height changes,  
837 *Science*, 301, 479–483, doi:10.1126/science.1084123, 2003b.
- 838 Santer, B. D., Painter, J. F., Mears, C. A., Doutriaux, C., Caldwell, P., Arblaster, J. M.,  
839 Cameron-Smith, P. J., Gillett, N. P., Gleckler, P. J., Lanzante, J., Perlwitz, J., Solomon, S.,

- 840 Stott, P. A., Taylor, K. E., Terray, L., Thorne, P. W., Wehner, M. F., Wentz, F. J., Wigley, T.  
841 M. L., Wilcox, L. J., and Zou, C.: Identifying human influences on atmospheric  
842 temperature, *Proc. Natl. Acad. Sci. USA*, 110(1), 26–33, 2013.
- 843 Sato, M., Hansen, J. E., McCormick, M. P., and Pollack, J. B.: Stratospheric aerosol optical  
844 depth, 1850-1990, *J. Geophys. Res.*, 98, 22 987–22 994, 1993.
- 845 Seidel, D. J. and Randel, W. J.: Variability and trends in the global tropopause estimated from  
846 radiosonde data. *J. Geophys. Res.*, 111, D21101, doi:10.1029/2006JD007363, 2006.
- 847 Sherwood, S. C., Meyer, C. L., Allen, R. J., and Titchner, H. A.: Robust tropospheric warming  
848 revealed by iteratively homogenized radiosonde data, *J. Climate*, 21, 5336–5350,  
849 doi:10.1175/2008JCLI2320.1, 2008.
- 850 Shine, K. P., Bourqui, M. S., Forster, P. M. de F., Hare, S. H. E., Langematz, U., Braesicke, P.,  
851 Grewe, V., Ponater, M., Schnadt, C., Smith, C. A., Haigh, J. D., Austin, J., Butchart, N.,  
852 Shindell, D. T., Randel, W. J., Nagashima, T., Portmann, R. W., Solomon, S., Seidel, D.  
853 J., Lanzante, J., Klein, S., Ramaswamy, V., and Schwarzkopf, M. D.: A comparison of  
854 model-simulated trends in stratospheric temperatures, *Q. J. R. Meteorol. Soc.*, 129, 1565–  
855 1588, doi:10.1256/qj.02.186, 2003.
- 856 Son, S.-W., Polvani, L. M., Waugh, D. W., Birner, T., Akiyoshi, H., Garcia, R. R., Gettelman,  
857 A., Plummer, D. A., and Rozanov, E.: The Impact of Stratospheric Ozone Recovery on  
858 Tropopause Height Trends, *J. Climate*, 22, 429–445, doi:10.1175/2008JCLI2215.1, 2009.
- 859 Staehelin, J., Harris, N.R.P., Appenzeller, C. and Eberhard, J.: Ozone trends: A review, *Rev.*  
860 *Geophys.*, 39(2), 231– 290, 2001.
- 861 Tiao, G.C., Reinsel, G.C., Xu, D., Pedrick, J.H., Zhu, X., Miller, A.J., DeLuisi, J.J., Mateer,  
862 C.L., Wuebbles, D.J.: Effects of autocorrelation and temporal sampling schemes on  
863 estimates of trend and spatial correlation, *J. Geophys. Res.*, 95, 20507–20517, 1990.
- 864 Thompson, D. W. J., and Solomon, S.: Recent stratospheric climate trends as evidenced in  
865 radiosonde data: Global structure and tropospheric linkages, *J. Climate*, 18, 4785–4795,  
866 2005.
- 867 Thompson, D. W. J. and Solomon, S.: Understanding recent stratospheric climate change, *J.*  
868 *Climate*, 22, 1934–1943, doi:10.1175/2008JCLI2482.1, 2009.
- 869 Thompson, D. W. J., Wallace, J. M., Kennedy, J. J., and Jones, P. D.: An abrupt drop in  
870 Northern Hemisphere sea surface temperature around 1970, *Nature*, 467,444–447,

- 871 doi:10.1038/nature09394, 2010.
- 872 Thompson, D. W. J., Seidel, D. J., Randel, W. J., Zou, C.-Z., Butler, A. H., Mears, C., Osso,  
873 A., Long, C., and Lin, R.: The mystery of recent stratospheric temperature trends, *Nature*,  
874 491, 692–697, doi:10.1038/nature11579, 2012.
- 875 Thorne, P. W., Parker, D. E., Tett, S. F. B., Jones, P. D., McCarthy, M., Coleman, H., and  
876 Brohan, P.: Revisiting radiosonde upper air temperatures from 1958 to 2002, *J. Geophys.*  
877 *Res.*, 110, D18105, doi:10.1029/2004JD005753, 2005.
- 878 Webb, W. L.: *Structure of the stratosphere and mesosphere*, New York and London (Academic  
879 Press), Pp. 380, 183 Figures, 1966.
- 880 Wild, M., Ohmura, A., and Makowski, K.: Impact of global dimming and brightening on  
881 global warming, *Geophys. Res. Lett.*, 34, L04702, doi:10.1029/2006GL028031, 2007.
- 882 WMO (World Meteorological Organization), *Scientific Assessment of Ozone Depletion:*  
883 *2010, Global Ozone Research and Monitoring Project–Report No. 52*, 516 pp., Geneva,  
884 Switzerland, 2011.
- 885 WMO (World Meteorological Organization), *Scientific Assessment of Ozone Depletion:*  
886 *2006, Global Ozone Research and Monitoring Project–Report No. 50*, 572 pp., Geneva,  
887 Switzerland, 2007.
- 888 Wu, J., Xu, Y., Yang, Q., Han, Z., Zhao, D., and Tang, J.: A numerical simulation of aerosols’  
889 direct effects on tropopause height, *Theor Appl Climatol*, 112, 659–671,  
890 doi:10.1007/s00704-012-0760-5, 2013.
- 891 Zerefos, C. S. and Mantis, H. T.: Climatic fluctuations in the Northern Hemisphere  
892 stratosphere, *Arch. Met. Geoph. Biokl., Ser. B*, 25, 33–39, 1977.
- 893 Zerefos, C. S., Bais, A. F., Ziomas, I. C., and Bojkov, R. D.: On the relative importance of  
894 quasi-biennial oscillation and El Nino/southern oscillation in the revised Dobson total  
895 ozone records, *J. Geophys. Res.*, 97, 10 135–10 144, doi:10.1029/92JD00508, 1992.
- 896 Zerefos, C. S., Tourpali, K., Eleftheratos, K., Kazadzis, S., Meleti, C., Feister, U., Koskela, T.,  
897 and Heikkilä, A.: Evidence of a possible turning point in solar UV-B over Canada,  
898 Europe and Japan, *Atmos. Chem. Phys.*, 12, 2469–2477, doi:10.5194/acp-12-2469-2012,  
899 2012.
- 900 Zou, C.-Z., Gao, M., and Goldberg, M. D.: Error structure and atmospheric temperature trends  
901 in observations from the Microwave Sounding Unit, *J. Climate*, 22, 1661–1681,

902        doi:10.1175/2008JCLI2233.1, 2009.

903

904

905

906 Table 1: Trend calculations in northern hemisphere summer (JJA) based on the monthly  
 907 normalised time series of the layer mean temperature ( $^{\circ}\text{C}/\text{decade}$ ) and tropopause pressure  
 908 (hPa/decade) calculated from NCEP reanalysis and filtered from natural variations at the  
 909 latitudinal belts a) 5 N-30 N, b) 30 N - 60 N and c) 60 N - 90 N. The layers are: L1: 1000-925  
 910 hPa, L2: 925-500 hPa, L3: 500-300 hPa, L4: 100-50 hPa and L5: 50-30 hPa. The trends  
 911 calculations refer to the periods 1958-1979, 1980-2001, 1980-2005 and 1980-2011.

912

913 Period 1958-1979

Layer	90-60N		60-30N		30-05N	
	Trend	t-test	Trend	t-test	trend	t-test
L1	.26 $\pm$ .11	2.48	-.01 $\pm$ .04	-.25	.11 $\pm$ .03	3.91
L2	.10 $\pm$ .09	1.12	-.11 $\pm$ .04	-2.92	-.01 $\pm$ .04	-.22
L3	-.42 $\pm$ .07	-5.69	-.25 $\pm$ .04	-6.89	-.11 $\pm$ .05	-2.19
L4	-.57 $\pm$ .31	-1.83	-.59 $\pm$ .06	-10.37	-.21 $\pm$ .12	-1.79
L5	-.77 $\pm$ .35	-2.19	-.74 $\pm$ .09	-8.38	-.59 $\pm$ .10	-5.99
<b>TP</b>	<b>1.98<math>\pm</math> 1.25</b>	<b>1.58</b>	<b>2.42<math>\pm</math> .28</b>	<b>8.57</b>	<b>.19<math>\pm</math> .24</b>	<b>.78</b>

914

915 Period 1980-2001

Layer	90-60N		60-30N		30-05N	
	Trend	t-test	Trend	t-test	trend	t-test
L1	.39 $\pm$ .11	3.42	.23 $\pm$ .04	5.31	.06 $\pm$ .03	2.00
L2	.05 $\pm$ .09	.56	.19 $\pm$ .04	4.74	.04 $\pm$ .04	.93
L3	.14 $\pm$ .08	1.83	.07 $\pm$ .04	1.50	-.10 $\pm$ .05	-2.20
L4	-.70 $\pm$ .34	-2.04	-.94 $\pm$ .07	-14.14	-.90 $\pm$ .11	-8.30
L5	-.66 $\pm$ .36	-1.84	-.83 $\pm$ .08	-10.02	-.73 $\pm$ .09	-8.20
<b>TP</b>	<b>-1.87<math>\pm</math> 1.69</b>	<b>-1.10</b>	<b>-1.59<math>\pm</math>.35</b>	<b>-4.52</b>	<b>-.82<math>\pm</math>.24</b>	<b>-3.43</b>

916

917 Period 1980-2005

Layer	90-60N		60-30N		30-05N	
	Trend	t-test	trend	t-test	trend	t-test
L1	.61 $\pm$ .09	6.75	.28 $\pm$ .03	8.31	.11 $\pm$ .02	5.51
L2	.14 $\pm$ .07	2.07	.24 $\pm$ .03	7.81	.11 $\pm$ .03	3.67
L3	.23 $\pm$ .06	3.91	.11 $\pm$ .03	3.20	-.01 $\pm$ .03	-.35
L4	-.43 $\pm$ .26	-1.61	-.69 $\pm$ .06	-11.86	-.79 $\pm$ .08	-9.51
L5	-.46 $\pm$ .28	-1.66	-.63 $\pm$ .07	-9.14	-.55 $\pm$ .08	-6.90
<b>TP</b>	<b>-1.06<math>\pm</math> 1.30</b>	<b>-.82</b>	<b>-.72<math>\pm</math>.27</b>	<b>-2.68</b>	<b>-.75<math>\pm</math>.18</b>	<b>-4.14</b>

918

919 Period 1980-2011

Layer	90-60N		60-30N		30-05N	
	Trend	t-test	Trend	t-test	trend	t-test
L1	.65 $\pm$ .07	9.18	.29 $\pm$ .03	10.83	.13 $\pm$ .02	7.85
L2	.25 $\pm$ .05	4.68	.27 $\pm$ .03	10.50	.16 $\pm$ .02	6.40
L3	.28 $\pm$ .05	5.99	.16 $\pm$ .03	5.91	.07 $\pm$ .03	2.22
L4	-.32 $\pm$ .22	-1.50	-.53 $\pm$ .05	-10.03	-.67 $\pm$ .07	-10.21
L5	-.38 $\pm$ .22	-1.70	-.45 $\pm$ .06	-7.59	-.41 $\pm$ .06	-6.51
<b>TP</b>	<b>-1.49<math>\pm</math> 1.07</b>	<b>-1.40</b>	<b>-1.07<math>\pm</math>.25</b>	<b>-4.23</b>	<b>-.91<math>\pm</math>.15</b>	<b>-5.92</b>

920

921

922

923

924 Table 2: Trend calculations in northern hemisphere summer (JJA) based on the monthly  
 925 normalised time series of the layer mean temperature ( $^{\circ}\text{C}/\text{decade}$ ) and tropopause pressure TP  
 926 (hPa/decade) calculated from the WACCM model and filtered from natural variations at the  
 927 latitudinal belts a) 5 N-30 N, b) 30 N - 60 N and c) 60 N - 90 N. The layers are: L1: 1000-925  
 928 hPa, L2: 925-500 hPa, L3: 500-300 hPa, L4: 100-50 hPa and L5: 50-30 hPa. The trends  
 929 calculations refer to the periods 1958-1979, 1980-2001 and 1980-2005.

930

931 Period 1958-1979

Layer	90-60N		60-30N		30-05N	
	Trend	t-test	trend	t-test	trend	t-test
L1	.70±.45	1.55	.01±.32	.02	-.02±.10	-.16
L2	.37±.09	4.23	-.01±.04	-.20	.19±.02	8.66
L3	.13±.06	2.14	.02±.04	.43	.24±.03	7.83
L4	-.26±.32	-.81	-.22±.10	-2.25	-.30±.09	-3.22
L5	-.28±.35	-.80	-.32±.13	-2.41	-.57±.10	-5.80
<b>TP</b>	<b>.33± 1.13</b>	<b>.29</b>	<b>-1.42±.45</b>	<b>-3.14</b>	<b>-.57±.53</b>	<b>-1.07</b>

932

933 Period 1980-2001

Layer	90-60N		60-30N		30-05N	
	Trend	t-test	trend	t-test	trend	t-test
L1	.14±.42	.33	.12±.36	.34	.40±.10	3.97
L2	.40±.10	3.90	.29±.04	6.67	.22±.04	5.14
L3	.33±.07	4.64	.26±.05	5.25	.29±.07	4.31
L4	-.43±.28	-1.50	-.16±.14	-1.19	-.31±.15	-2.08
L5	-.35±.31	-1.13	-.40±.17	-2.40	-.44±.16	-2.73
<b>TP</b>	<b>-2.20± 1.02</b>	<b>-2.16</b>	<b>-.75±.43</b>	<b>-1.74</b>	<b>-.10±.53</b>	<b>-1.19</b>

934

935 Period 1980-2005

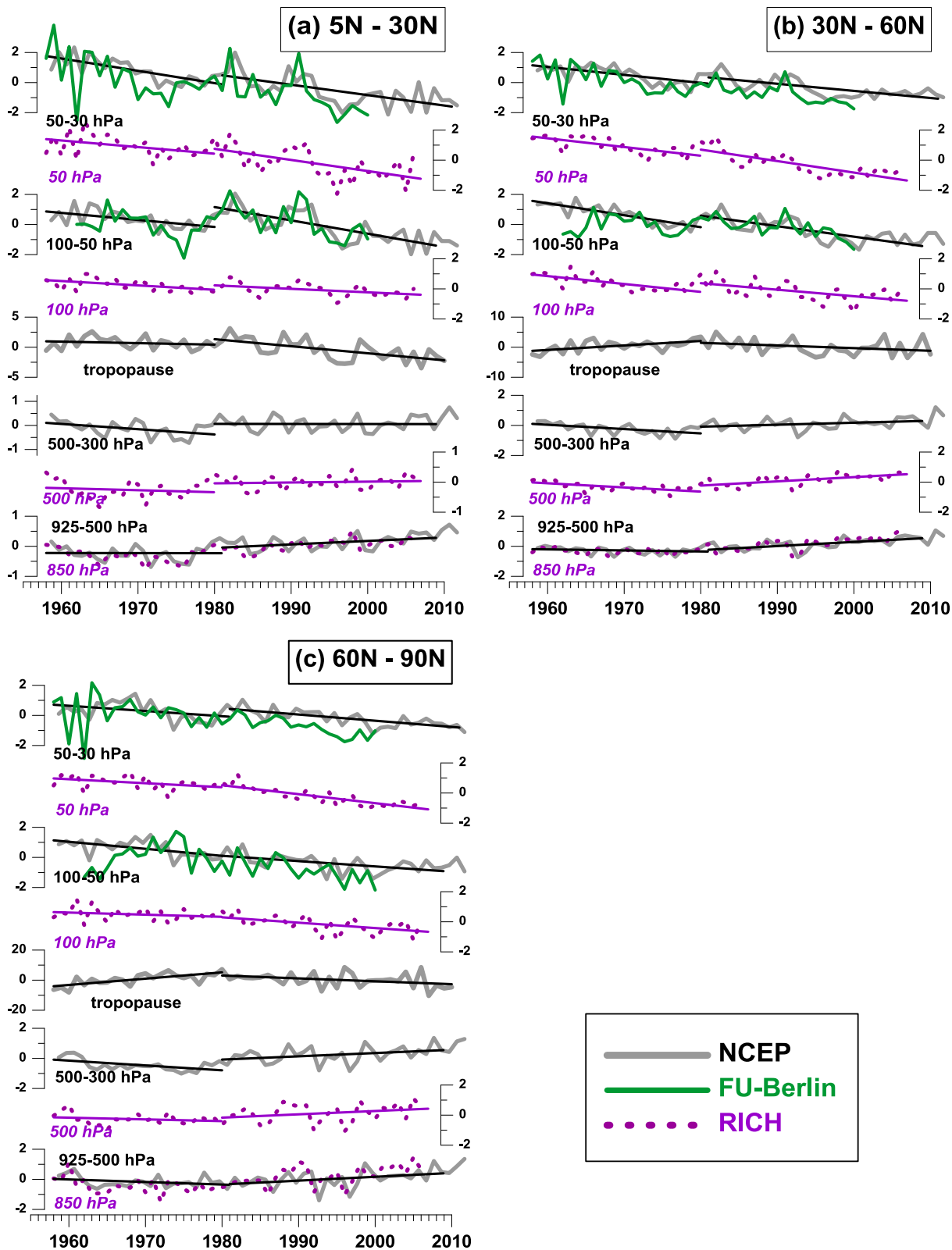
Layer	90-60N		60-30N		30-05N	
	Trend	t-test	trend	t-test	trend	t-test
L1	.04±.32	.12	-.03±.29	-.11	.35±.08	4.43
L2	.34±.08	4.40	.31±.04	8.39	.23±.03	7.49
L3	.30±.06	5.39	.32±.04	7.83	.32±.05	6.46
L4	-.52±.23	-2.30	-.13±.10	-1.28	-.23±.11	-2.14
L5	-.46±.25	-1.85	-.34±.13	-2.72	-.30±.11	-2.62
<b>TP</b>	<b>-2.87±.86</b>	<b>-3.35</b>	<b>-.69±.34</b>	<b>-2.01</b>	<b>-.55±.40</b>	<b>-1.38</b>

936

937

938

939  
940  
941



942  
943

944  
945  
946

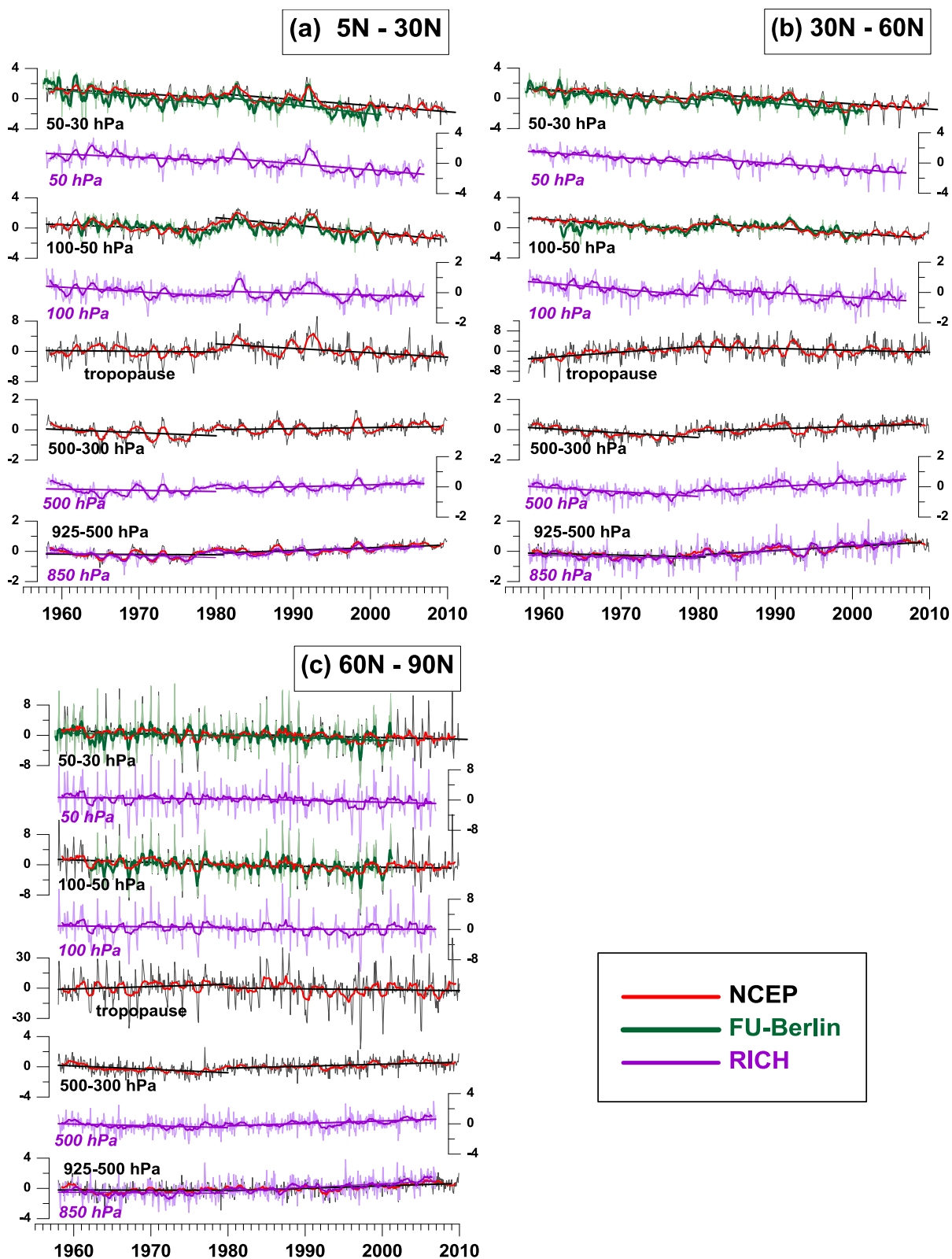
947 Figure 1: Layer mean temperature variations in northern hemisphere summer (JJA) at layers

948 925-500 hPa, 500-300 hPa, 100-50 hPa and 50-30 hPa calculated from NCEP reanalysis and  
949 FU-Berlin datasets and filtered from natural variations for three latitudinal belts a) 5N-30N, b)  
950 30N - 60N and c) 60N - 90N. The respective summer normalised time series of temperature  
951 from RICH dataset at levels 850 hPa, 500 hPa, 50 hPa and 30 hPa are also illustrated as well  
952 as the NCEP tropopause pressure. The trends lines before and after 1979 are superimposed.  
953 Grey lines denote NCEP reanalysis variations. Green lines denote variations as depicted in the  
954 FU-Berlin analysis, while purple dotted lines the RICH data temperature. The units at vertical  
955 axis are in degrees °C except for the tropopause that is in hPa.

956

957

958  
959



960  
961

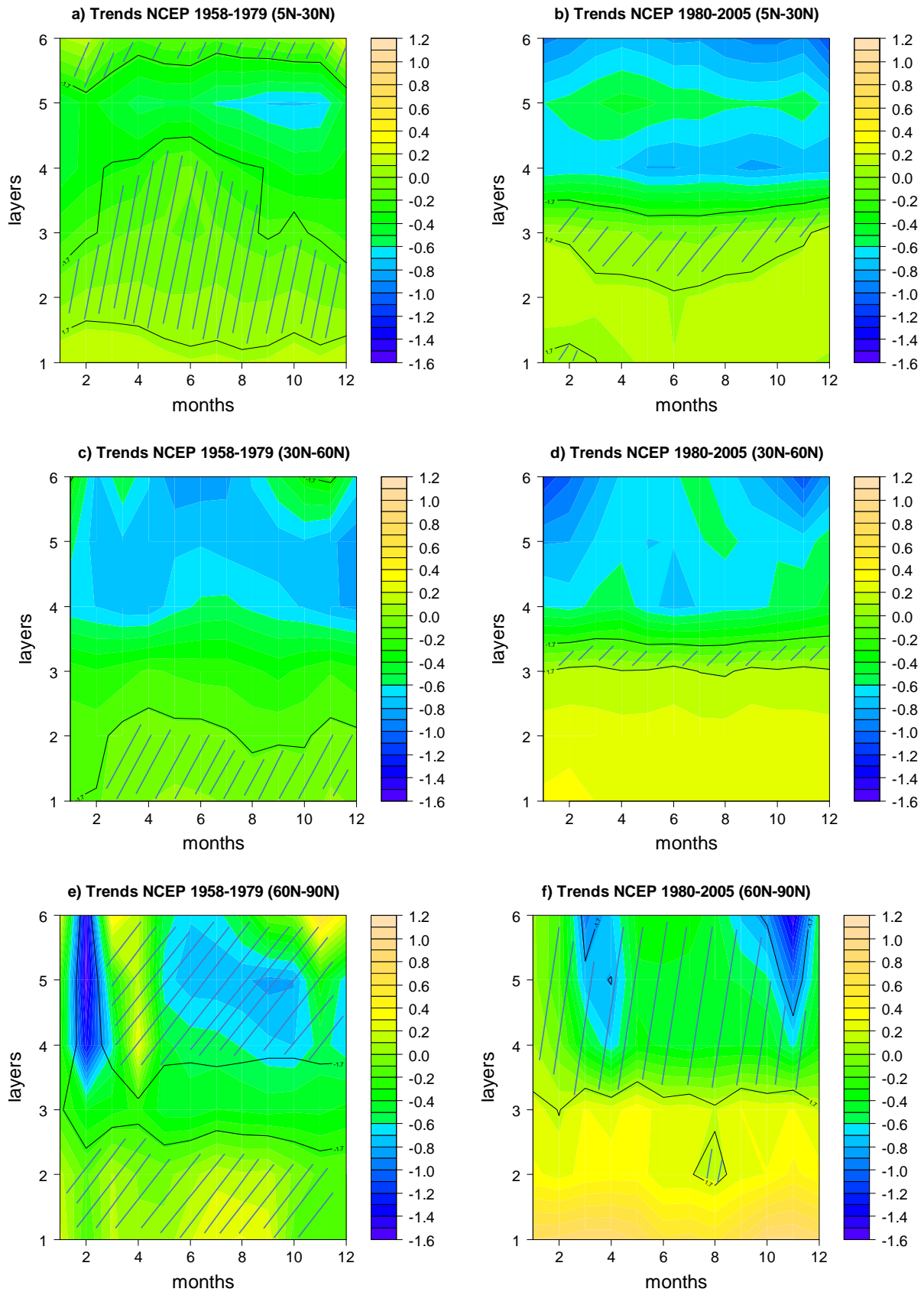
962  
963  
964

965 Figure 2: Monthly normalised time series of the layer mean temperature at layers 925-500 hPa,  
966 500-300 hPa, 100-50 hPa and 50-30 hPa calculated from NCEP reanalysis and FU-Berlin

967 datasets for the northern hemisphere and filtered from natural variations at the latitudinal belts  
968 a) 5 N-30 N, b) 30 N - 60 N and c) 60 N - 90 N. The respective monthly normalised time  
969 series of temperature from RICH dataset at levels 850 hPa, 500 hPa, 50 hPa and 30 hPa are  
970 also illustrated with purple lines as well as the NCEP tropopause pressure normalized monthly  
971 means. The trends lines before and after 1979 are also superimposed. The units at vertical axis  
972 are in degrees °C except for the tropopause that is in hPa.

973

974

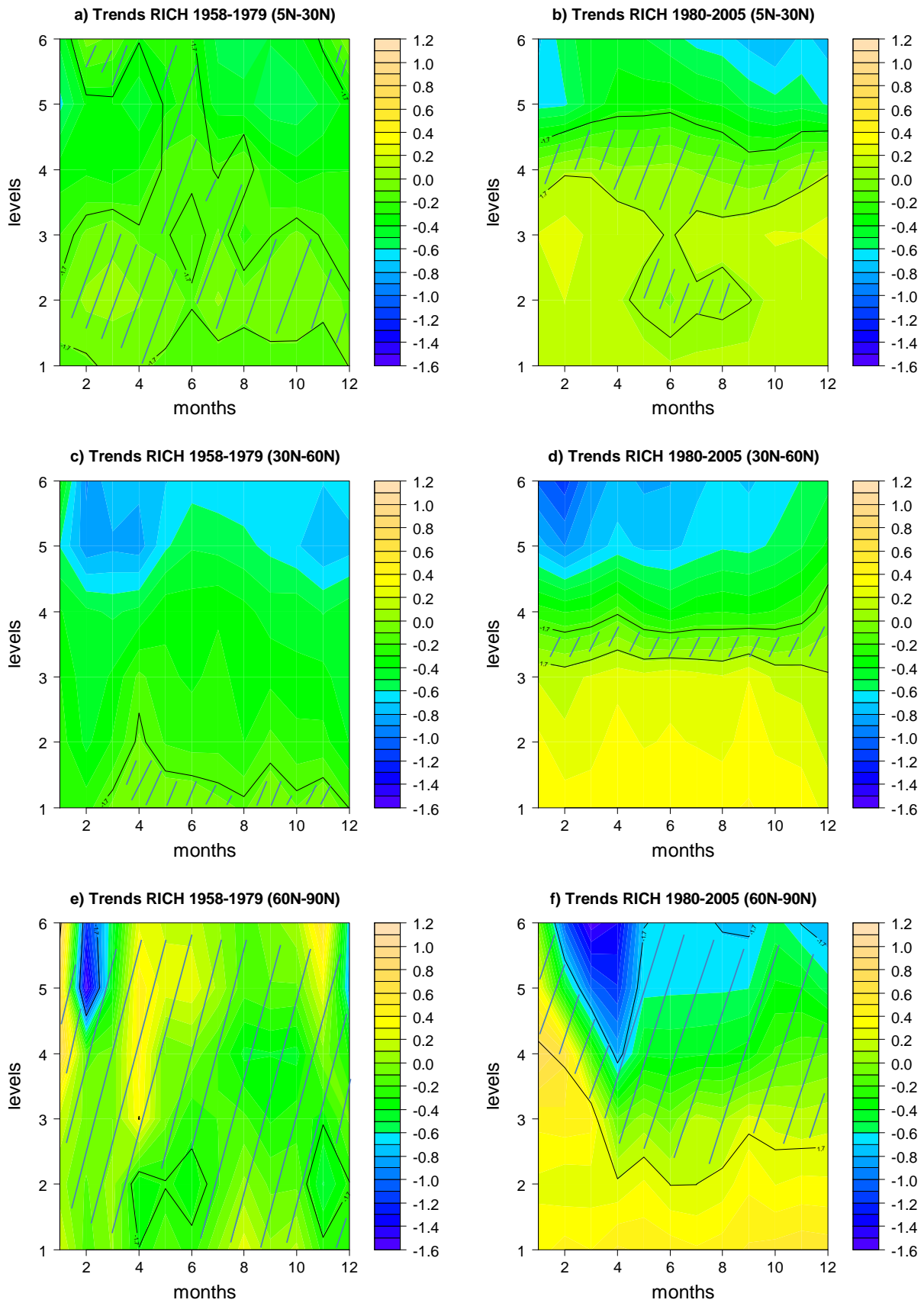


975

976 Figure 3: Layer mean temperature trends ( $^{\circ}\text{C}/\text{decade}$ ) for each month (x-axis) and layer (y-  
 977 axis) based on NCEP reanalysis over the periods 1958-1979 and 1980-2005, respectively, for

978 three latitudinal belts a) and b) for 5N-30N, c) and d) for 30N - 60N and e) and f) for 60N -  
979 90N. The layers are: Layer 1: 1000-925 hPa, Layer 2: 925-500 hPa, Layer 3: 500-300 hPa,  
980 Layer 4: 100-50 hPa, Layer 5: 50-30 hPa, and Layer 6: 30-10 hPa. The shaded areas are non-  
981 statistically significant at 90% confidence level.

982



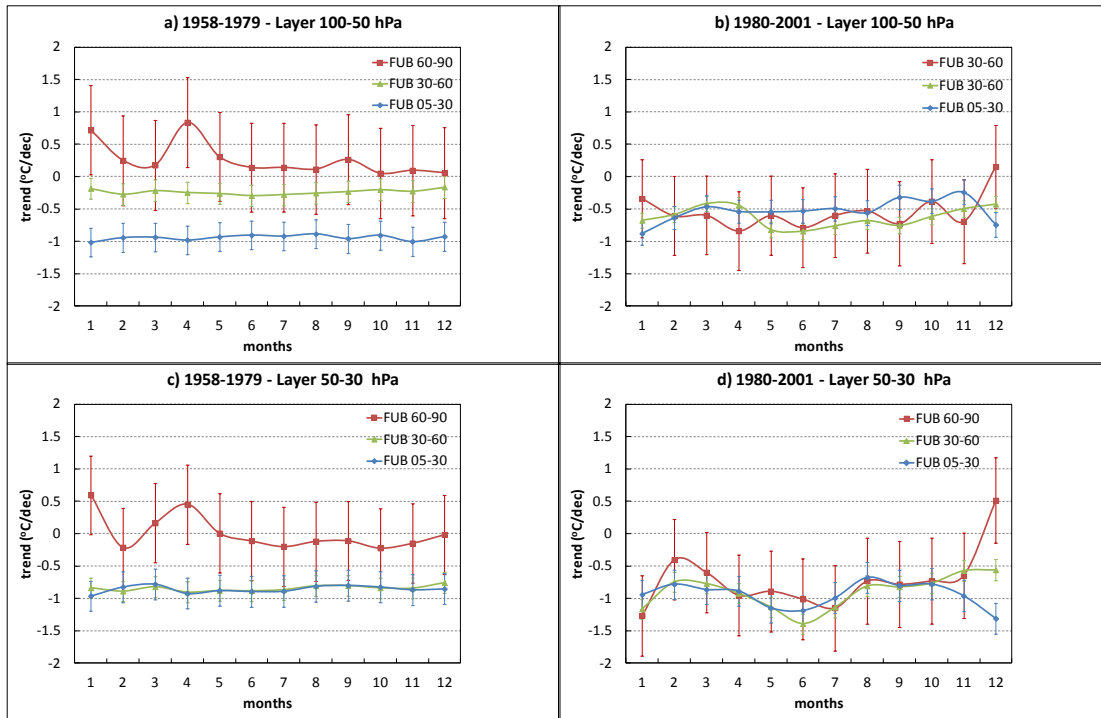
983

984 Figure 4: Temperature trends (°C/decade) for each month (x-axis) and level (y-axis) based on

985 RICH dataset over the periods 1958-1979 and 1980-2005, respectively, for three latitudinal

986 belts a) and b) for 5N-30N, c) and d) for 30N - 60N and e) and f) for 60N - 90N. The levels  
987 are: Level 1: 850 hPa, Level 2: 500 hPa, Level 3: 300 hPa, Level 4: 100 hPa, Level 5: 50 hPa,  
988 and Level 6: 30 hPa. The shaded areas are non-statistically significant at 90% confidence  
989 level.  
990

991



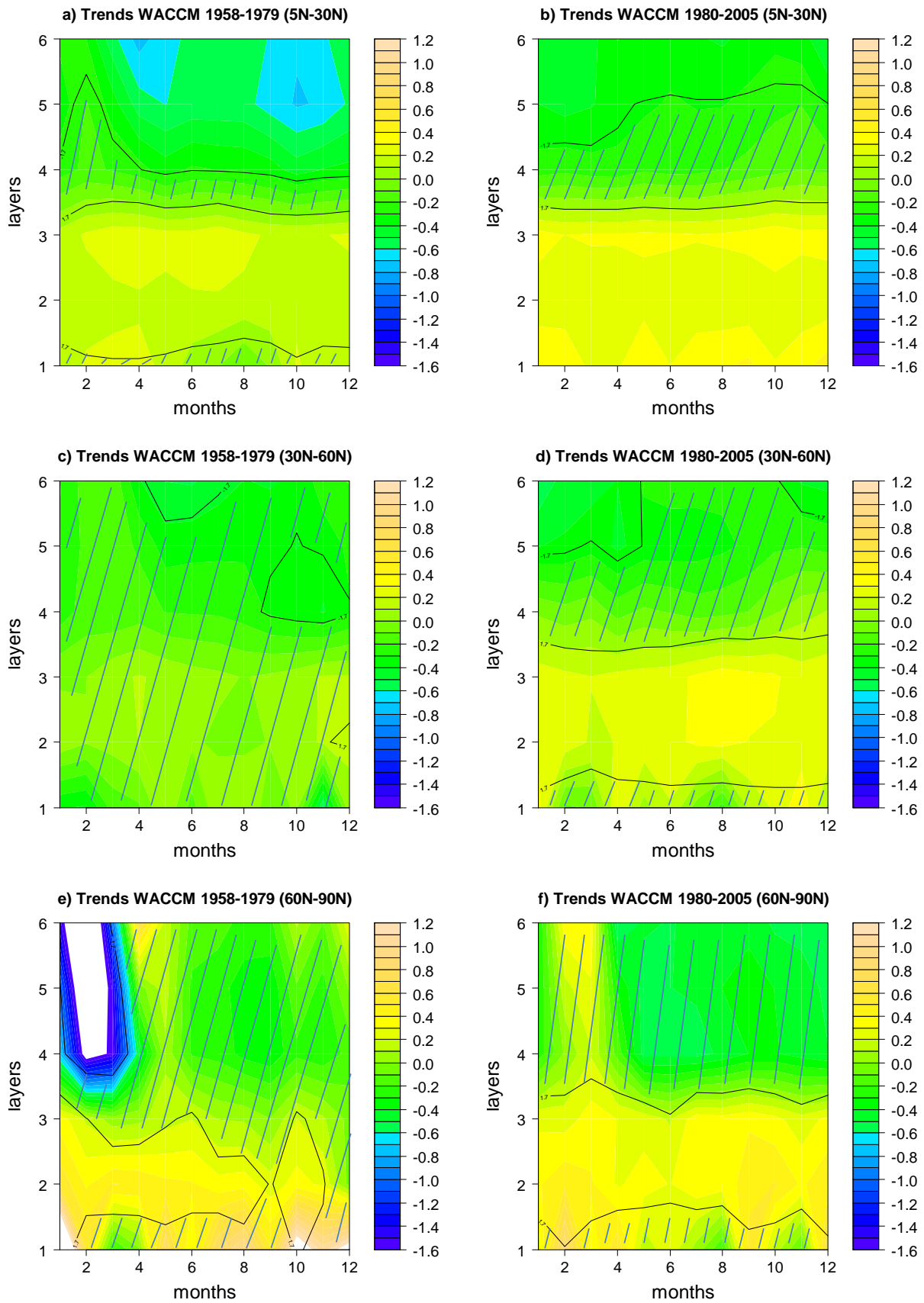
992

993

994 Figure 5: Mean temperature trends ( $^{\circ}\text{C}/\text{decade}$ ) for each month (x-axis) based on FU-Berlin  
 995 dataset over the periods 1958-1979 and 1980-2001 for the layers 100-50 hPa (a and b) and 50-  
 996 30 hPa (c and d) for the three latitudinal belts, 5N-30N (blue), 30N - 60N (green) and 60N -  
 997 90N (red).

998

999



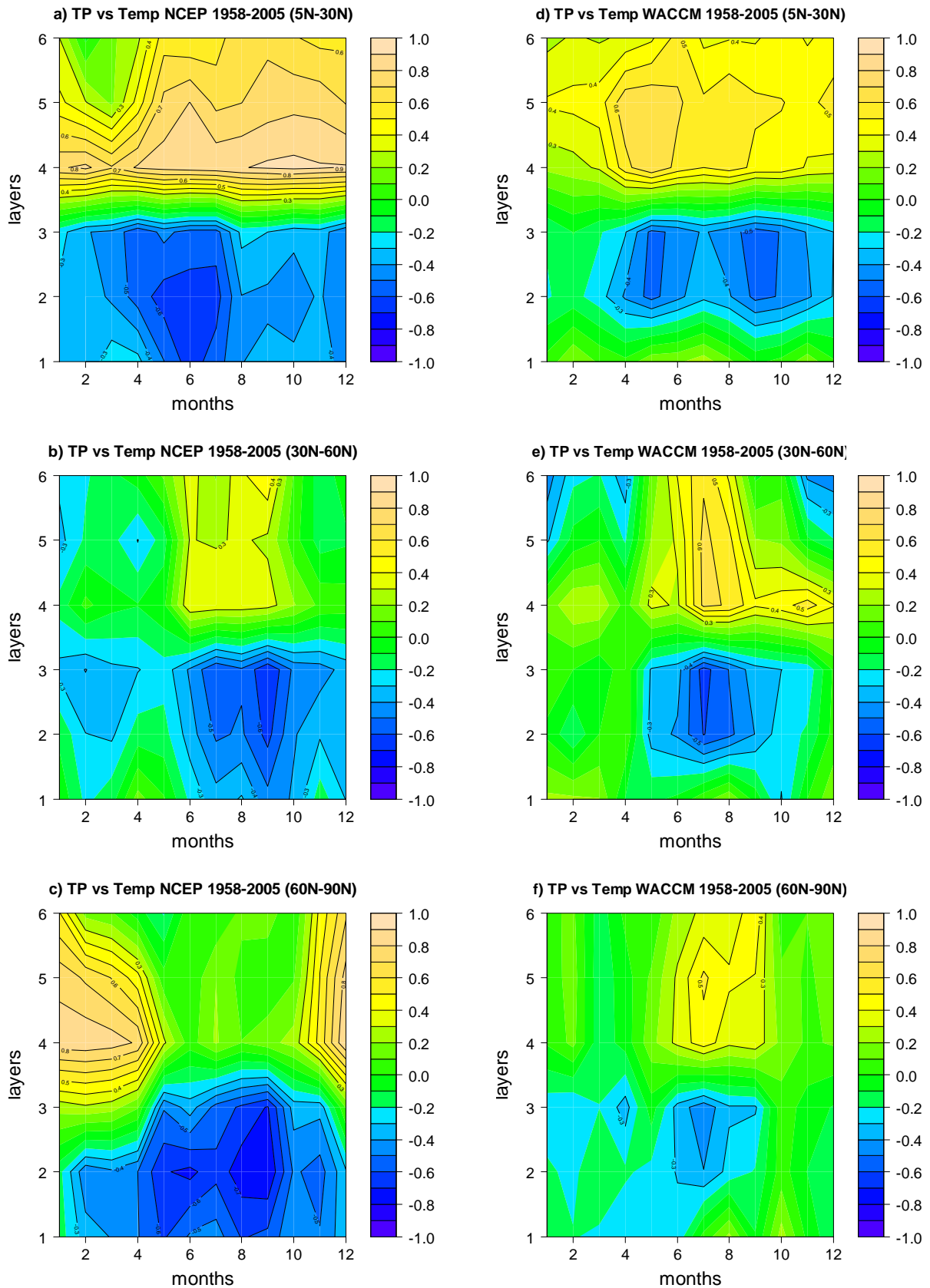
1000

1001 Figure 6: Layer mean temperature trends ( $^{\circ}\text{C}/\text{decade}$ ) for each month (x-axis) and layer (y-

1002 axis) based on WACCM model over the periods 1958-1979 and 1980-2005, respectively, for

1003 three latitudinal belts a) and b) for 5N-30N, c) and d) for 30N - 60N and e) and f) for 60N -  
1004 90N. The layers are: Layer 1: 1000-925 hPa, Layer 2: 925-500 hPa, Layer 3: 500-300 hPa,  
1005 Layer 4: 100-50 hPa, Layer 5: 50-30 hPa, and Layer 6: 30-10 hPa. The shaded areas are non-  
1006 statistically significant at 90% confidence level.

1007



1008

1009

1010

1011

Figure 7: Correlation plots between tropopause pressure and layer mean temperature for each month (x-axis) and layer (y-axis) based on NCEP reanalysis (left panel) and WACCM model (right panel) over the common period 1958-2005 for the three latitudinal belts: 5N-30N (a and

1012 d), 30N - 60N (b and e) and 60N - 90N (c and f). The layers are: Layer 1: 1000-925 hPa,  
1013 Layer 2: 925-500 hPa, Layer 3: 500-300 hPa, Layer 4: 100-50 hPa, Layer 5: 50-30 hPa, and  
1014 Layer 6: 30-10 hPa. The contours indicate the statistically significant correlations at 95%  
1015 significance level with  $\rho > 0.3$  or  $\rho < -0.3$ .

1016

1017